Geomorphology

Plio-Pleistocene drainage reorganization in the middle Yellow River of China, revealed by provenance and paleocurrent analysis of fluvial sediments

--Manuscript Draft--

Manuscript Number:	GEOMOR-13062R1
Article Type:	VSI: Fluvial archives
Keywords:	Yellow River; Detrital zircon; Drainage evolution; planation surface
Corresponding Author:	Zhenbo Hu, Doctor Lanzhou University Lanzhou, Gansu CHINA
First Author:	Menghao Li
Order of Authors:	Menghao Li
	Zhenbo Hu
	Ping Wang
	Baotian Pan
	David Bridgland
	Qinhong Mo
	Xiaohua Li
	Zijuan Dong
	Meiling Zhong
	Renzhe Pan
	Ningyi Li
Abstract:	Continental-scale drainage reorganization is generally understood to result from landform evolution forced by the coupling between tectonic activity and climate change, attracting worldwide attention. Planation surfaces and river terraces constitute the most direct geomorphological archives for integrating the history of river systems and for reconstructing processes of drainage reorganization based on provenance analysis of the fluvial sediments. The Middle Yellow River has incised into the Ordos Block, which was previously levelled by a planation surface, creating the Jinshaan Gorge and linking the Hetao Basin to the north and the Fenwei Basin to the south. Multiple lines of evidence, from terraces correlation, sedimentary characteristics, and fluvial provenance, suggest that the Middle Yellow River catchment was occupied by fluvio-lacustrine systems before drainage integration, accumulating a sedimentary sequence derived from surrounding Red Clay and bedrocks during the period between 8.3 and 3.7 Ma. The planation surface was uplifted subsequently, forcing reorganization of the fluvio-lacustrine systems. Their integration resulted in the formation of the Jinshaan Gorge prior to 1.2 Ma. Numerous terraces were created during incision by the Middle Yellow River from north to south along the gorge. Our data, obtained from zircon U-Pb dating and lithological composition of fluvial gravels, further points to a remarkable discrepancy in provenance between the fluvio-lacustrine systems overlying the planation surface and the terraces sequence formed by the integrated Middle Yellow River, confirming the drainage reorganization process constrained by the geomorphic records.

- Fluvio-lacustrine systems occupied the Middle Yellow River before integration.
- Yellow River terraces are different from fluvio-lacustrine systems in provenance.
- The Middle Yellow River has been excavated and integrated during Plio–Pleistocene.

Abstract

Continental-scale drainage reorganization is generally understood to result from landform evolution forced by the coupling between tectonic activity and climate change, attracting worldwide attention. Planation surfaces and river terraces constitute the most direct geomorphological archives for integrating the history of river systems and for reconstructing processes of drainage reorganization based on provenance analysis of the fluvial sediments. The Middle Yellow River has incised into the Ordos Block, which was previously levelled by a planation surface, creating the Jinshaan Gorge and linking the Hetao Basin to the north and the Fenwei Basin to the south. Multiple lines of evidence, from terraces correlation, sedimentary characteristics, and fluvial provenance, suggest that the Middle Yellow River catchment was occupied by fluvio-lacustrine systems before drainage integration, accumulating a sedimentary sequence derived from surrounding Red Clay and bedrocks during the period between 8.3 and 3.7 Ma. The planation surface was uplifted subsequently, forcing reorganization of the fluvio-lacustrine systems. Their integration resulted in the formation of the Jinshaan Gorge prior to 1.2 Ma. Numerous terraces were created during incision by the Middle Yellow River from north to south along the gorge. Our data, obtained from zircon U-Pb dating and lithological composition of fluvial gravels, further points to a remarkable discrepancy in provenance between the fluvio-lacustrine systems overlying the planation surface and the terraces sequence formed by the integrated Middle Yellow River, confirming the drainage reorganization process constrained by the geomorphic records.

Plio-Pleistocene drainage reorganization in the middle Yellow River of China, revealed by provenance and paleocurrent analysis of fluvial sediments

Menghao Li[1], Zhenbo Hu[1,2,3*], Ping Wang[4*], Baotian Pan[1,2,3], David Bridgland[5], Qinhong Mo[1], Xiaohua Li[1], Zijuan Dong[1], Meiling Zhong[1], Renzhe Pan[1], Ningyi Li[1]

[1] Key Laboratory of Western China's Environmental Systems (Ministry of Education), College of Earth and Environmental Sciences, Lanzhou University, Lanzhou, 730000, China.

[2] Institute of Green Development for the Yellow River Drainage Basin, Lanzhou University, Lanzhou, 730000, China.

[3] Shiyang River Basin Scientific Observing Station of Gansu Province, Lanzhou, 730000, China.

[4] School of Geography, Nanjing Normal University, Nanjing, 210023, China.

[5] Department of Geography, Durham University, Lower Mountjoy, South Road, Durham DH1 3LE, United Kingdom of Great Britain and Northern Ireland

Corresponding author: Zhenbo Hu (~~zhbhu@lzu.edu.cn~~zhbhu@lzu.edu.cn), Ping Wang (~~tigerwp@njnu.edu.cn~~tigerwp@njnu.edu.cn)

Formatted: Default Paragraph Font, Font: (Default) +Body (DengXian), 10.5 pt, (Asian) Chinese (PRC)

Formatted: Default Paragraph Font, Font: (Default) +Body (DengXian), 10.5 pt, (Asian) Chinese (PRC)

Formatted: Default Paragraph Font, Font: (Default) +Body (DengXian), 10.5 pt, (Asian) Chinese (PRC)

Formatted: Default Paragraph Font, Font: (Default) +Body (DengXian), 10.5 pt, (Asian) Chinese (PRC)

Abstract

Continental-scale drainage reorganization is generally understood to result from landform evolution forced by the coupling between tectonic activity and climate change, attracting worldwide attention. Planation surfaces and river terraces constitute the most direct geomorphological archives for integrating the history of river systems and for reconstructing processes of drainage reorganization based on provenance analysis of the fluvial sediments. The Middle Yellow River has incised into the Ordos Block, which was previously levelled by a planation surface, creating the Jinshaan Gorge and linking the Hetao Basin to the north and the Fenwei Basin to the south. Multiple lines of evidence, from terraces correlation, sedimentary characteristics, and fluvial provenance, suggest that the Middle Yellow River catchment was occupied by fluvio-lacustrine systems before drainage integration, accumulating a sedimentary sequence derived from surrounding Red Clay and bedrocks during the period between 8.3 and 3.7 Ma. The planation surface was uplifted subsequently, forcing reorganization of the fluvio-lacustrine systems. Their integration resulted in the formation of the Jinshaan Gorge prior to 1.2 Ma. Numerous terraces were created during incision by the Middle Yellow River from north to south along the gorge. Our data, obtained from zircon U-Pb dating and lithological composition of fluvial gravels, further points to a remarkable discrepancy in provenance between the fluvio-lacustrine systems overlying the planation surface and the terraces sequence formed by the integrated Middle Yellow River, confirming the drainage reorganization process constrained by the geomorphic records.

1. Introduction

As a peneplain is regenerated by elevation into a new cycle of life, a planation surface initiates a renewed cycle of erosion (Davis, 1899), marking the replacement of pre-existing drainage systems by new deeply incised river valleys at lower levels. Following a century-long debate on the mechanisms that generate planation surfaces (Strahler, 1950; King, 1953; Orme, 2013), investigations conducted by geomorphologists have significantly advanced the understanding of geomorphic evolution and river development associated with planation events in recent decades (Evenstar et al., 2014; Bar~~,~~ et al., 2016; Guillocheau et al., 2018).

Numerous investigations have been undertaken to constrain the initiation of planation-surface dissection chronologically by analyzing the youngest stratigraphic layers incised by the planation surface and determining the age of the oldest overlying sediments (Pan et al., 2012; Bar et al., 2016; Xiong et al., 2018). These endeavors aim to establish a timeframe for the genesis of the landscapes observable presently. The extensively distributed Tangxian-period planation surfaces in China have emerged as a prominent subject of investigation within this field of research. The Tangxian-period planation surface extends along the western periphery of the North China Plain, stretching between the Taihang and Lü~~u~~liang Mountains, and continues further onto the primary plateau surface of the Ordos Plateau (Pan et al., 2012; Hu et al., 2017; Xiong et al., 2018). Based on previous investigations, the formation of this planation surface probably commenced at 20 Ma, with sea level acting as the ultimate erosion base level (Li, 1999). The process involved weathering and erosion of the positive terrain, along with sedimentation filling the negative terrain, ultimately leading to the development of a peneplain-like landscape. The beginning of the dissection of the planation surface occurred at approximately 3.7 Ma as a consequence either of tectonic uplift or climate change, leading to the formation of the modern Yellow River and its tributaries (Li, 1991; Pan et al., 2011; Pan et al., 2012). However, the mechanisms and processes driving this landscape transformation remain debated.

The current scholarly deliberations revolve around two key aspects of this landscape history: first, the initial drainage pattern during the development of the peneplain before the formation of the Jinshaan Gorge section of the Yellow River and, second, the formation of the modern river system after the dissection of the planation surface. To address the above questions, considerable efforts have been devoted to the Tangxian-period planation surface and the downstream sedimentary basin (Pan et al., 2011, 2012; Hu et al., 2016; Xiong et al., 2018; Liu ~~et al.~~, 2020; Zhang et al., 2021; Li et al., 2022). Nevertheless, divergent interpretations arising from inconsistencies in materials or methods have led to a multitude of different patterns in drainage reorganization being hypothesized. To shed light on the process of drainage reorganization in the middle reaches of the Yellow River, this paper proposes an innovative approach that integrates comparative analysis of geomorphic surfaces and examination of the provenance of the overlying sediments.

This investigation focuses on the Baode section, a significant site extensively studied in relation to the Tangxian-period planation surface and the Neogene Red Clay in the middle reaches of the Yellow River (Zhu et al., 2008; Pan et al., 2011; Shang et al., 2016; Bohm et al., 2023). During the peneplanation period, the Baode region exhibited negative topography, with the surrounding endorheic drainage converging in a Baode paleolake (Pan et al., 2011). The center of lacustrine sediment accumulation was in the area of Luzigou, with a gradual decline in sediment thickness observed towards the lake edge. Simultaneously, the adjacent terrain experienced differential erosion, resulting in the removal of higher elevations and the deposition of Neogene aeolian Red Clay in areas that were comparatively lower and characterized by gentle slopes (Yue et al., 2007). The Neogene aeolian Red Clay divide into the Baode Red Clay (older than ~5.34 Ma) and Jingle

Red Clay at ~5.34 Ma (Zhu et al., 2008). Furthermore, remnants of gravel deposits are present on the planation surface, covered by Jingle Red Clay, and previous investigations have conjectured that these can be attributed to the endorheic drainage system during the peneplanation period (Pan et al., 2011, 2012). In terms of spatial distribution, these gravel units exhibit a parallel alignment with the Yellow River channel, extending across both sides of the modern valley. They resemble gravels associated with the Yellow River, but their lithological composition is relatively uncomplicated and distinct from these. In this study, we focus on the lithological composition and paleocurrents of these gravel units, comparing them with the sediments of the Baode paleolake and the Yellow River terraces, revealing a drainage system rerouted by a capture event. In addition, detrital zircon U–Pb chronology provenance studies of the Luzigou section and the Yellow River terraces have provided further information on the palaeo-hydrological pattern and evolutionary history of the Yellow River system.

2. Regional setting

2.1 General geology

The Ordos Block and the Lüliang Mountains are integral components of the North China Craton, comprising Archean and Paleoproterozoic metamorphic basement rocks that underwent reactivation and reconstruction during the Yanshanian orogeny (~137 Ma). The Ordos Block, formerly which was the Ordos Basin prior to the Cenozoic, was the scene of sediment accumulation from the Proterozoic to the Mesozoic (H. Peng et al., 2023). Exhumation and deformation occurred between the Eocene and the Late-Miocene, transforming the Ordos Block into a plateau. This was brought about by the northeastward growth of the Tibetan Plateau, which also led to the formation of initial faulted basins along the periphery of the Ordos Plateau (Shi et al., 2020). Following gradual uplift during the Yanshanian orogeny, the Lüliang Mountains were strongly uplifted during the Late Miocene (Zhao et al., 2016; Huang et al., 2021). Simultaneously, the faulted basins along the margins of the Ordos Plateau were further extended. These basins record sedimentary archives from the Eocene onwards and additionally serve as erosional base levels for the local drainage systems (Lu et al., 2023).

Starting in the Late Miocene, aeolian sediments have been deposited unconformably above the original landform, which may have suffered erosion by local fluvial or slope processes, with accumulation of residues in the lowlands (Yue et al., 2007). The deposition of Red Clay was initiated in the western piedmont of the Lüliang Mountains approximately 7 Ma, although differences in the age of its lower boundary are observed across multiple profiles, potentially associated with variations in the original landform (Xu et al., 2009; Ao et al., 2017; Sun et al., 2022). Between 3.7 and 2.6 Ma, typical aeolian sediments with a high mass magnetic susceptibility are present. Aeolian accumulation is linked to the overall uplift of the Tangxian-period peneplain and the complete isolation of some profiles from aqueous environments (Pan et al., 2011). In the Quaternary, a thick series of loess deposits accumulated continuously above the Red Clay, leading to the formation of the Chinese Loess Plateau, a prominent feature of the region's geological landscape (Liu et al., 2015).

2.2 Geographic setting

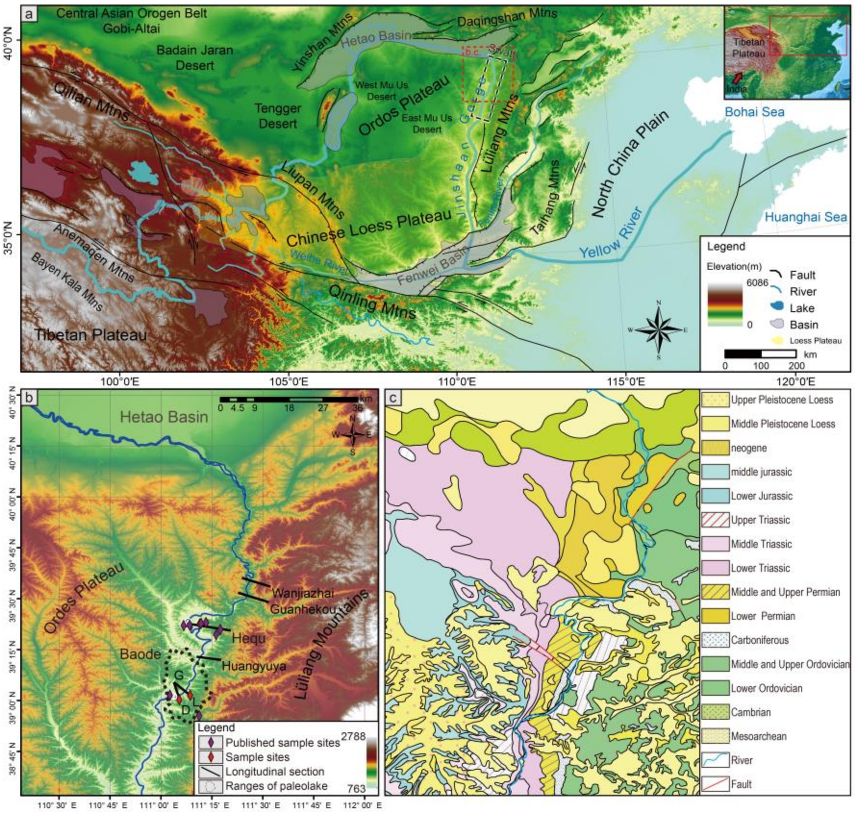
a
Central Asian Orogen Belt
Gobi-Altai
Badain Jaran Desert
Qilian Mtns
Tengger Desert
Yinshan Mtns
Hetao Basin
Daqingshan Mtns
West Mu Us Desert
Ordos Plateau
East Mu Us Desert
Lüliang Mtns
Taihang Mtns
North China Plain
Bohai Sea
Huanghai Sea
Liupan Mtns
Chinese Loess Plateau
Weihe River
Fenwei Basin
Qinling Mtns
Yellow River
Anemaqen Mtns
Bayen Kala Mtns
Tibetan Plateau
India
Legend
Elevation(m)
6086
0
Fault
River
Lake
Basin
Loess Plateau
km
0 100 200
40°0'N
35°0'N
100°0'E
105°0'E
110°0'E
115°0'E
120°0'E
b
Hetao Basin
Ordes Plateau
Wanjiazhai
Guanhekou
Hequ
Baode
Huangyuya
Lüliang Mountains
Legend
Published sample sites
Sample sites
Longitudinal section
Ranges of paleolake
2788
763
c
Upper Pleistocene Loess
Middle Pleistocene Loess
neogene
middle jurassic
Lower Jurassic
Upper Triassic
Middle Triassic
Lower Triassic
Middle and Upper Permian
Lower Permian
Carboniferous
Middle and Upper Ordovician
Lower Ordovician
Cambrian
Mesoarchean
River
Fault

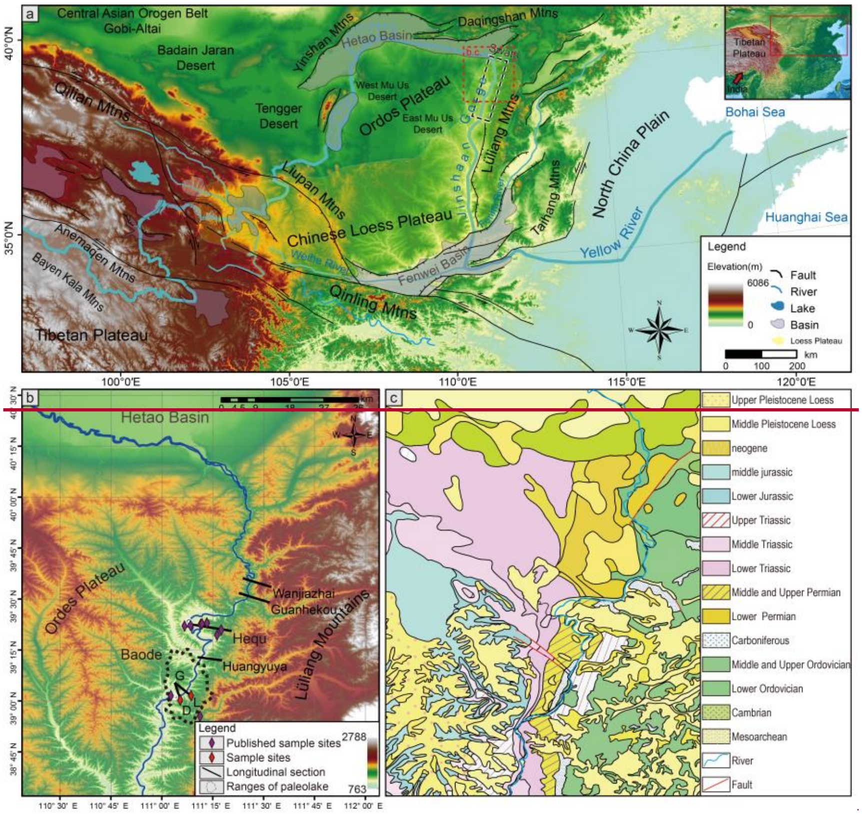

Figure 1. Topographic map, sampling sites, and geological map. a.) The Yellow River flows from the Tibetan ~~plateau~~Plateau, makes a U-shaped bend through the Hetao ~~basin~~Basin, cuts through the Jinshaan Gorge, runs eastward across the Fenwei ~~basin~~Basin, and finally reaches the North China Plain and flows into the Bohai Sea. b.) The longitudinal geomorphic sections and ~~S~~sampling sites studied for detrital zircon U–Pb dating in this and previous research are shown in different colors. (G: Gaojiayinze, D: Dayandun, L: Luzigou) c.) Stratigraphic units of varying geological epochs are delineated with different colors.

The present-day topography of the Ordos Plateau is characterized by higher elevations in the west and lower elevations in the east (Fig 1). At the western piedmont of the Lüliang Mountains, the elevation reaches approximately 1000 m. Originating from the northeastern Tibetan Plateau, the Yellow River follows a U-shaped bend within the Hetao Basin before flowing from north to south into the Fenwei Basin, passing through the western piedmont of the Lüliang Mountains. The section from the outlet of the Hetao Basin to the entrance of the Fenwei Basin is commonly referred to as the Jinshaan Gorge section of the Yellow River, which is notable for its deep valleys, high mountains, and rugged terrain. In conjunction with the deeply incised canyon, the Jinshaan Gorge encompasses several depressions that exhibit lower elevations compared to the Ordos Plateau, about 650~850 m. These depressions have facilitated the widening of the Yellow River valley and the development of local strath areas. Previous studies have speculated that these depressions might have been lakes during the peneplanation period, which were distributed sporadically along the Jinshaan Gorge and were later connected by the headward erosion of the Yellow River (Pan et al., 2011).

The considerable accumulation of aeolian sediments within the region serves as an exceptional repository of climatic information (Ao et al., 2017; Peng et al., 2018). A previous study investigated the fluctuations in goethite concentration within aeolian sediments at the Chaona profile on the Chinese Loess Plateau, revealing a distinct pattern of intensified East Asian Summer Monsoons, featuring augmented precipitation, during the Late Miocene to Early Pleistocene (Zhang et al., 2017). This intensified monsoonal activity probably contributed to increased surface runoff and expedited landscape evolution processes.

3. Geomorphic sequences and sedimentary characteristics along the northern Jinshaan Gorge

The top of the Baode paleolake sedimentary sequence is unconformably overlain by Red Clay and subsequent loess, at altitude comparable with those at which the aeolian sequences overlies weathered limestone bedrock. The uppermost fluvio-lacustrine Baode deposits, together with the weathering crusts capping the limestone, form the main body of the Tangxian-period planation surface (Pan et al., 2011). Investigation of the Baode paleolake has centered on the analysis of cross sections between Gaojiayinze and Luzigou (G–L) and between Gaojiayinze and Dayandun (G–D), with extensive fieldwork. By establishing connections between the boundary of the fluvio-lacustrine deposit with the bedrock, a rough estimation of the spatial extent of the Baode paleolake was obtained.

Our fieldwork along the Yellow River channel from south to north up to the Hetao Basin revealed that remnants of river gravels and overlying Red Clay are commonly distributed above the northern Jinshaan gorge. They are situated on or slightly below the level of the Tangxian-period planation surface, at an elevation is close to the top of the fluvio-lacustrine deposition in the Baode area. We found that the gravels can be divided into two distinct units at different elevations, G1 (the lower one) and G2 (Fig. 2).

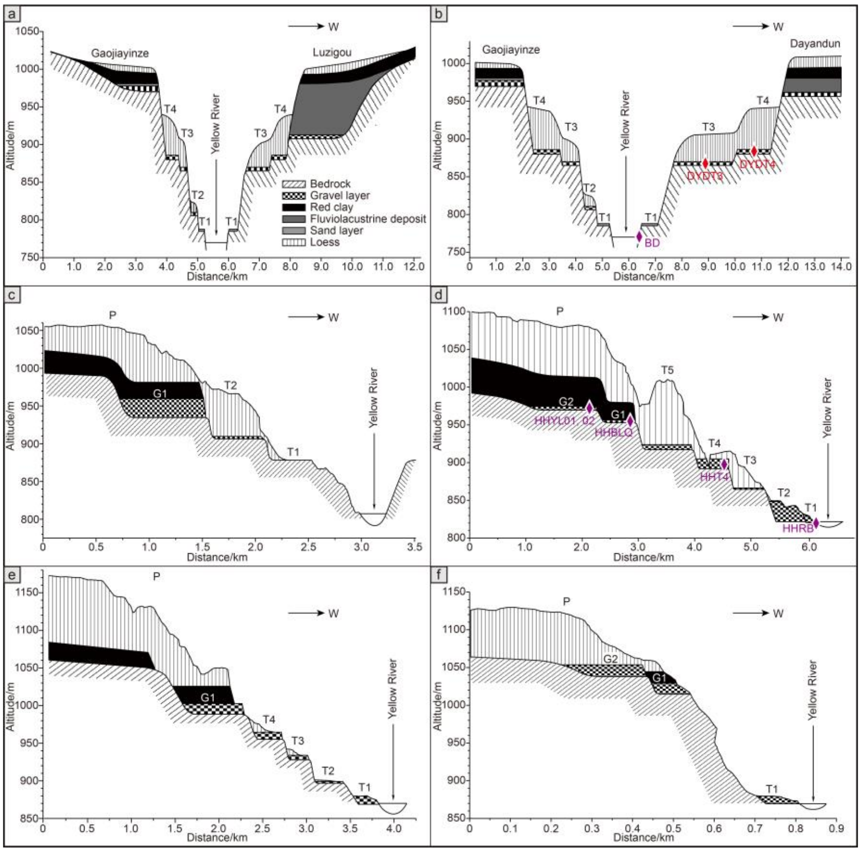

Figure 2. Schematic cross-section of fluvial terraces along the Jinshaan Gorge (see **Fig.1b** for location). a.) Gaojiayinze–Luzigou (G–L) section, b.) Gaojiayinze–Dayandun (G–D) section, c.) Huangyuya section, d.) Hequ section, e.) Guanhekou section, f.) Wanjiazhai section. Sample sites and published sites marked by red and purple diamonds respectively.

The uppermost surface of the higher gravel unit (G2) is 184~~∼~~150 m above the level of the Yellow River. This gravel layer is 5 m thick and is overlain by 4 m of overbank silt and then up to 28 m of Red Clay. This sequence is capped by aeolian loess, characteristic of the region. The gravel clasts range between 2 and 10 cm diameter, with limestone being the dominant lithology, and shows clear imbrication. Magnetostratigraphic dating of the lowermost Red Clay accumulation above the gravel establishes that its formation predates ~4.9 Ma (Pan et al., 2011), indicating a minimum age for the gravel.

The top of the lower (G1) gravel is 160–133 m above the level of the Yellow River. This gravel is 2 m in thick and is overlain by about 15 m of Red Clay, with a further cover of aeolian loess. The gravel clasts are generally 2–7 cm, again are mainly limestone, with an imbricated arrangement. The bas~~e~~al of Red Clay above the G1 gravel is dated to 3.7 Ma (Pan et al., 2011).

Three longitudinal sections, named after Huangyuya, Guanhekou, and Wanjiazhai, were carefully traced along these two gravel units from the Baode paleolake in the south to the Hetao Basin in the north (Fig. 1b, Fig. 2). We conducted measurements of the gravel units' surface elevation for each section, relative to the river. These measurements were then compared with the G–L, G–D, and Hequ sections, which were previously published, allowing a comprehensive assessment of the morphological consistency within the studied region. Two terraces are preserved below the G1 gravel in the Huangyuya section, both of which are strath terraces with Quaternary loess directly overlying their gravels. The Guanhekou section preserves a total of four Yellow River terraces. While the lowest (T1) is a fill terrace, the remainder are strath terraces, with subsequent deposition of Quaternary loess. In the Wanjiazhai section, only a single fill terrace is preserved.

Preservation of the G1 and G2 gravel and the more recent Yellow River terraces does not occur uniformly across all sections. However, a Swath plot reveals that, despite the variations, these features exhibit significant comparability, leaving no doubt that they collectively represent geomorphic records of rivers oriented in a north-south direction. In order to validate whether they belong to a singular river system, we undertook further investigations.

4. Material and methods

4.1 Investigation and ~~Sampling~~ sampling sites

To reconstruct the evolution of the drainage system, first, the establishment of a comprehensive chronological framework is essential and, second, an analysis of sediment composition is crucial for revealing the source–sink pattern. The study area benefits from previous paleomagnetic dating (Pan et al., 2011), which has successfully established a robust chronological framework for the aeolian sediments deposited above the gravels. Nonetheless, there remains a lack of quantitative investigations concerning the lithological composition and provenance of these gravels.

We investigated the following sections (from south to north, respectively) in detail: G–L (39°01′21″ N,111°09′38″E), G–D (38°58′41″N,111°05′21″E), Huangyuya (39°07′26″N,111°10′44″E), Hequ (39°23′20″N,111°08′13″E), Guanhekou (39°29′32″N,111°24′39″E), and Wanjiazhai (39°34′08″ N,111°25′59″E). The elevation and thickness of the gravel bodies and of overlying overbank and aeolian sediments were measured using high-precision differential GPS (Trimble GEO 7X). The Hequ section has been studied previously for gravel lithology and zircon U–Pb chronology (Xiong et al., 2022), and our present study extends these investigations to encompass each section located at the northern extremity of the Jinshaan Gorge, employing both analysis of gravel lithology and paleocurrent measurement. Furthermore, recent provenance studies of the middle and lower reaches of the Yellow River using zircon U–Pb chronology have provided much evidence for the reconstruction of drainage evolution (Kong et al., 2014; Nie et al., 2015; Xiao et al., 2020; Zhang et al., 2021). In our present study, we conducted a provenance study for the fluvio-lacustrine deposits in the Luzigou section and the Yellow River terrace sediments in the G–D section.

As previously described, the Luzigou section (39°01′21″N,111°09′38″E) is the sedimentary center of the Baode paleolake, where fluvio-lacustrine deposits have accumulated since the Late Miocene (Pan et al., 2011), attaining a thickness of up to 77 m, stacked unconformably above the underlying Carboniferous sandstone (Fig. 3). At their base is a distinct set of fluvial gravel unit, measuring approximately 10 m in thickness. These gravels are highly abraded, predominantly showing a sub-rounded morphology, with clast diameters 2–10 cm. Their lithological composition is exceptionally homogeneous, with nearly 98% limestone. They are distinctly imbricated and incorporate mud lenses, signifying that they represent fluvial deposition with stable channels. Sample LZGD was taken at the bottom of this gravel layer. The overlying fluvio-lacustrine strata primarily comprise mudstone, siltstone, and sandstone, with a cumulative thickness of ~67 m. Notably, another distinct gravel unit, which is inset into the fluvio-lacustrine sequence and with the same lithology as G2 found on the planation surface, occurs 30 m below the top surface with a thickness of 3 m. Along the profile, from the bottom upwards, we collected detrital samples LZG11, LZG9, LZG8 and LZG6 (Fig. 3). Based on previous chronological investigations, the ages of LZGD, LZG11, LZG9, LZG8, and LZG6 correspond to paleomagnetic ages of approximately 10 Ma, 7.1 Ma, 5.2 Ma, 4.9 Ma, and 3.7 Ma, respectively (Pan et al., 2011).

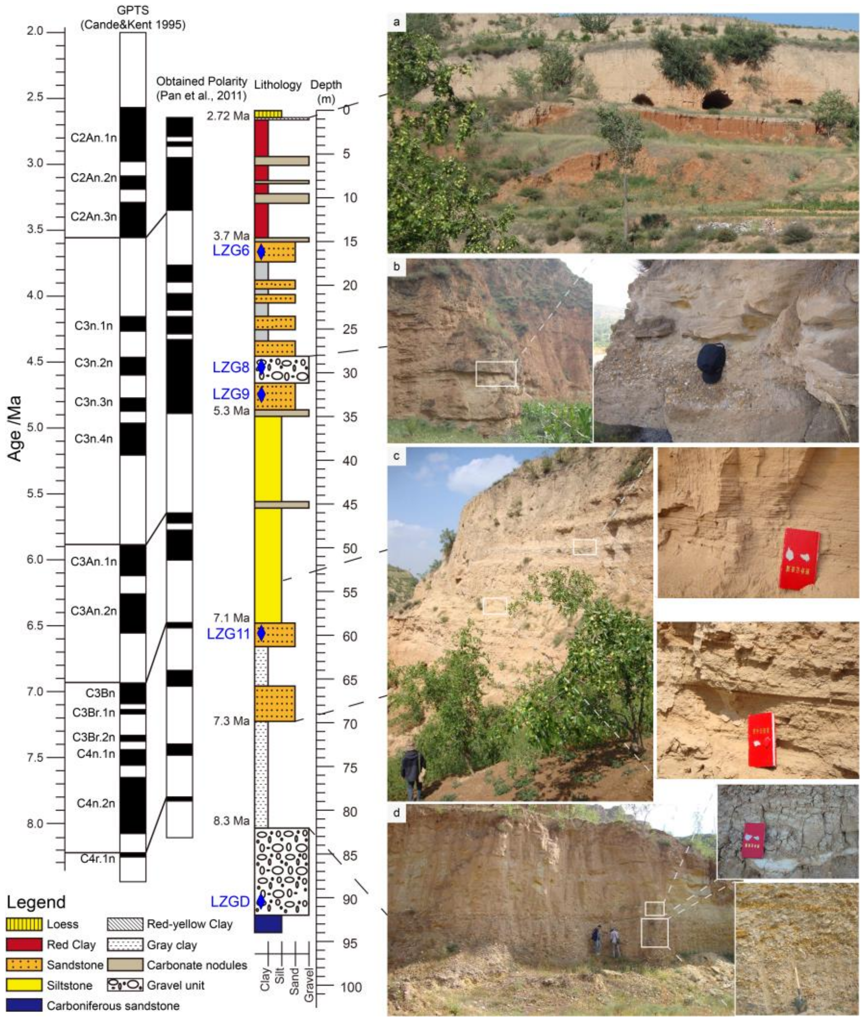

Figure 3. Magnetostratigraphy, pedostratigraphy and field photos of the Luzigou section in the Baode area. Zircon U–Pb samples location marked by pale green diamonds. a.) The loess–Red Clay boundary. b.) The higher gravel unit. c.) Two sand layers in the middle section. d.) Lacustrine strata and lowest gravel unit in the basal section. For chronological framework, lithological description, and interpreted chrons (black and white for normal and reverse geomagnetic polarities) for see Pan et al. (2011).

4.2 Sedimentary analyses

We measured the lithological composition of the G1 and G2 gravels across all sections, as well as for the gravel unit within the Baode fluvio-lacustrine sequence. Additionally, paleocurrent were measured in the G1 and G2 gravels in the Huangyuya, Hequ, Guanhekou, and Wanjiazhai sections, as well as within the Yellow River terrace gravels in the Hequ section. The lithology and preferred orientation (imbrication) of >100 gravel clasts were measured for each sample, which was observed on the gravel unit outcrops. The size range of measured clasts is >3 cm in b-aixs. The gravel-forming geology and resultant clast lithologies in the study area are relatively homogeneous, primarily comprising limestone, sandstone, quartzite, quartzitic sandstone, mudstone, slate, and phyllite. To obtain imbrication, we measured the inclinations of the a-b surfaces of the gravel clasts, which corresponds to the upstream direction, and plotted the rose diagrams and preferred orientation using the software PC99 (Woolfe et al., 2000). Figure 4 shows three-dimensional pie charts depicting the distribution of gravel lithology, as well as paleocurrent rose diagrams (in which flow direction is denoted by the red arrow).

4.3 Detrital zircon pretreatment

Samples were wet sieved to isolate the 15–250 μm fraction, from which zircon grains were separated using standard dense-liquid techniques. Zircon grains were randomly selected under a binocular microscope and mounted using epoxy resin. Pretreatment was carried out at the Key Laboratory of Mineral Resources in Western China (Gansu Province), School of Earth Sciences, at Lanzhou University, China.

4.4 U–Pb geochronological measurement

Detrital-zircon dating was carried out by means of inductively coupled plasma mass spectrometry (ICP-MS) using an Agilent 7700x instrument with an attached CETAC Analyte –Excite Excimer Laser Ablation System, at the Department of Geography, Nanjing Normal University, China. The laser beam diameter was set to 20 μm and, as standard reference materials, zircon 91500 (Wiedenbeck et al., 1995), GJ- 1(Jackson et al., 2004), Plešovice (Sláma et al., 2008), and QH (Li et al., 2009) were used. For zircons younger than 1000 Ma, we used $^{206}Pb/^{238}U$ ages, whereas $^{206}Pb/^{207}Pb$ ages were used for zircons older than 1000 Ma, with uncertainties expressed at 2σ. Samples with >10% discordance were not considered (see full data provided as Supplementary Material).

Data are presented as kernel density estimation plots (KDEs) and non-matrix multi-dimensional scaling (MDS) maps, using the software IsoplotR (Vermeesch, 2012, 2013), were used for provenance interpretation.

5. Results

5.1. Lithological composition and paleocurrents

Data on gravel clast lithology, paleocurrent and elevation profiles of geomorphic surfaces were combined and plotted on the Swath diagram of the northern Jinshaan Gorge (Fig. 4). The lithological composition of gravels within the Baode paleolake sequence and the high-level G1 and G2 gravels is predominantly limestone, exhibiting a more homogeneous distribution in the southern section of the study area. This lithological pattern changes to sandstone, quartzitic sandstone, and quartzite components in the northern section. In contrast, the lithological composition of Yellow River gravels in the Hequ section shows a gradual but progressive change in composition from the higher to lower terraces with sandstone, quartzite and limestone, significantly differing from the lithology observed in G1, G2 and Baode paleolake gravels with predominant limestone.

This notable dissimilarity is further highlighted in the paleocurrent patterns. The inclinations of the a-b surfaces of the gravel clasts within the Yellow River terraces predominantly exhibit a single direction towards the north, suggesting consistent paleoflow from north to south, ~~comforming~~ conforming with the present-day course of the Yellow River. In contrast, the inclinations of the a-b surfaces of the G1 and G2 gravel clasts display a relatively mixed distribution, with a predominant southward trend. This indicates a reversal of drainage in comparison with the modern Yellow River.

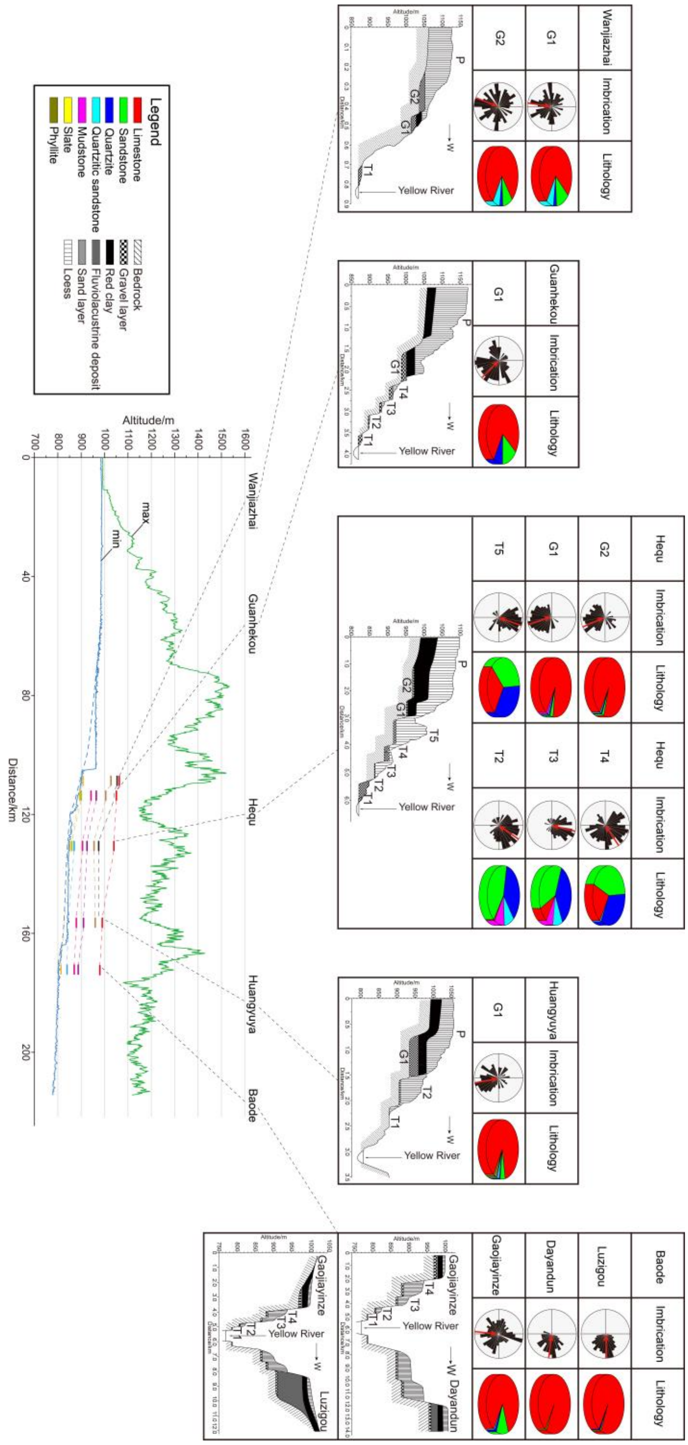

Legend
Limestone
Sandstone
Quartzite
Quartzitic sandstone
Mudstone
Slate
Phyllite
Bedrock
Gravel layer
Red clay
Fluviolacustrine deposit
Sand layer
Loess
Altitude/m
Distance/km
max
min
Wanjiazhai
Guanhekou
Hequ
Huangyuya
Baode
Imbrication
Lithology
Yellow River
Gaojiayinze
Dayandun
Luzigou

Figure 4. The 3D pie charts showing gravel clast lithology, rose diagrams showing paleocurrent directions, and elevation profiles of geomorphic surfaces, all plotted onto the Swath diagram of the northern Jinshaan Gorge of the Yellow River. Maximum and minimum elevation along a 25-km-wide swath window (perpendicular to swath transect), the location of which is shown in Fig 1a.

5.2. Zircon U–Pb chronological spectrum

KDE plots are utilized to illustrate the zircon U–Pb spectrum (Fig. 5). In order to facilitate the analysis, our samples are plotted alongside those of previous authors, allowing comprehensive comparison and examination of the data. Sample LZGD shows dominant peaks at ~2500 Ma, and minor peaks at ~250 Ma and ~2500 Ma. Sample LZG11 has subequal dominant peaks at ~250 Ma and ~450 Ma, with minor peaks at ~800 Ma, ~1800 Ma and ~2500 Ma. Sample LZG9 displays dominant peaks at ~250 Ma and ~1800 Ma, a lower peak at ~450 Ma, and minor peaks at ~800 Ma and ~2500 Ma. Sample LZG8 and LZG6 show dominant peaks at ~1800 Ma, and lower peaks at ~250 Ma and ~2500 Ma. The Yellow River terraces (samples from DYDT4 and DYDT3) display subequal peaks at ~1800 Ma, ~250 Ma, and ~2500 Ma, like the spectrum of Yellow River terrace T4 in Hequ (HHT4).

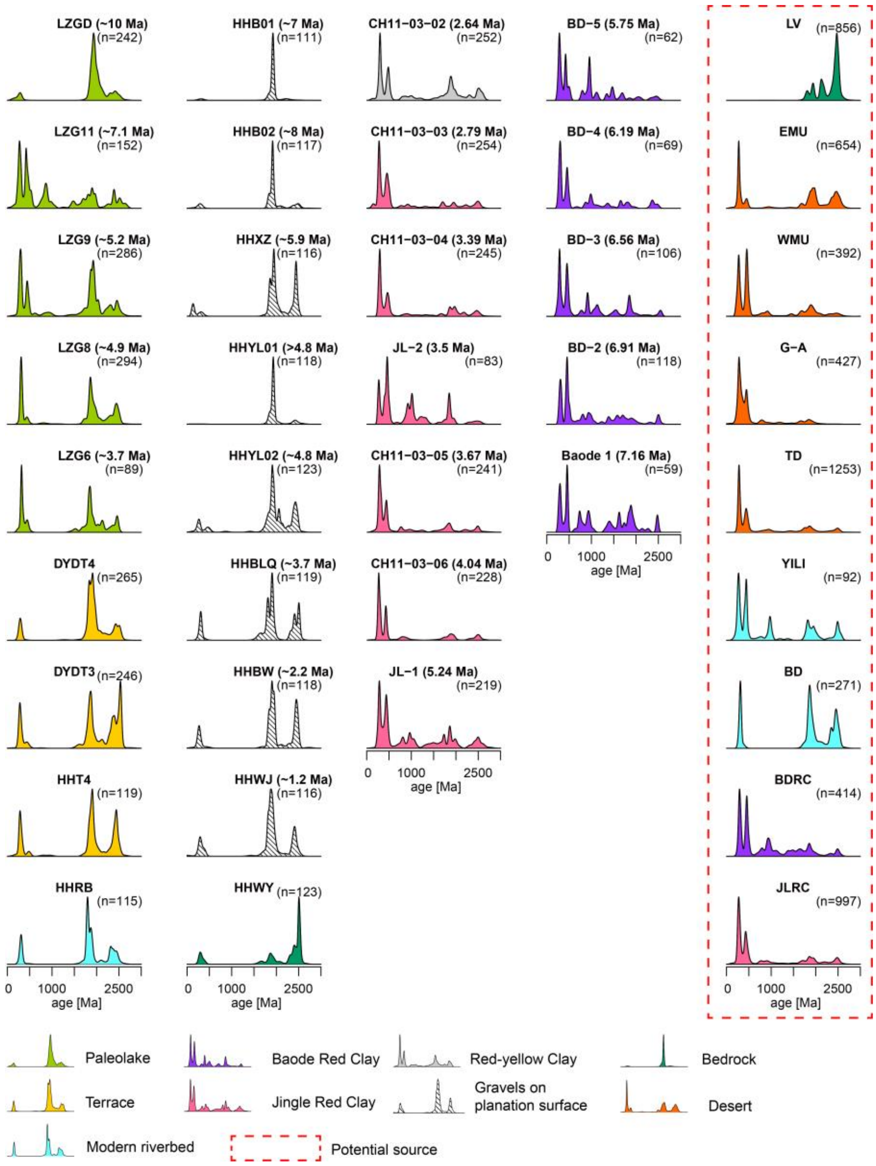

Figure 5. KDE plots of U–Pb zircon-age data, published data from Zhao et al. (2008), Stevens et al. (2010, 2013), Liu et al. (2011), Liu et al. (2012), Wang et al. (2014), Nie et al. (2015), Licht et al. (2016), Shang et al. (2016), Zhang et al. (2016, 2021), Xiong et al. (2022), Bohm et al. (2023) (full datasets provided as Supplementary Material).

6. Discussion

6.1 Drainage reconstruction on the planation surface

Gravel fabric analysis has been widely employed in fluvial evolution studies within sedimentary records of river terraces (Rust, 1972; Miao et al., 2008; Souza et al., 2022). The rose diagrams provide valuable insights into local paleocurrents, indicating that a river different from the modern Yellow River flowed from south to north across the study area during the peneplanation period. The chronological analysis of the G2 gravel unit suggests that this river system existed during the early Pliocene (minimum age 4.9 Ma). The sediment chronology of the Hetao Basin reveals deposition in the eastern part of the basin since at least the Late Miocene, with a hiatus indicated by an unconformity dated ~5.3 Ma (Shi et al., 2020). On the basis of the aforementioned evidence, we propose that the process of drainage integration events began at this time, with the fluvial outflow from the Baode paleolake, prior to which this was probably a long-term endorheic lacustrine system. The Yellow River traversed the Hetao Basin prior to entering the Jinshaan Gorge, depositing gravels and coarse sands from the upper reaches (Nie et al., 2015), and the gravels within the gorge predominantly originate from the adjacent mountainous regions. Specifically, these gravels comprise limestone sourced from the Ordovician strata of the Lüliang Mountains, while the sandstone predominantly originated from the Triassic and Cretaceous strata of the Ordos block.

Zircon KDE plots can provide valuable insights into drainage evolution, revealing similar patterns indicated by the gravel-forming geology and resultant clast lithologies (Fig. 5). The LZGD samples exhibit striking similarities to samples HHB01, HHB02, and HHYL01 of Xiong et al. (2022), which suggests a common provenance from the Lüliang Mountain. This observation aligns with the low-temperature thermal age evidence in indicating rapid uplift of the Lüliang Mountains at ~12 Ma

(Zhao et al., 2016). It is highly likely that the uplift of the Lüliang Mountains, coupled with the extensive lateral river system in the western piedmont, facilitated the deposition of these gravels in lower parts of the peneplain. This deposition is also evident in the Liulin area within the middle Jinshaan Gorge (Li et al., 2009).

A distinct variation in provenance is evident between LZGD and LZG11, with the latter displaying a more diverse spectrum characterized by peaks at ~250, ~450, ~800, and ~2500 Ma. No zircon spectra like LZG11 were found in sediment samples from the geomorphic surfaces in the Hequ section. However, it is noteworthy that the sample LZG11 exhibits remarkable similarities to the Late Miocene Red Clay deposits in the Baode area (Shang et al., 2016; Bohm et al., 2023). This multi-peak pattern probably signifies the presence of materials originating from the Central Asian Orogen Belt and transported over long distances by East Asian Winter Monsoon. The chronologies of multiple sedimentary sequences suggest that aeolian deposition to the east of the Liupan Mountains may have commenced around 7 Ma (Sun et al., 2022). The sample LZG11 represents a period characterized by increased aridification in inland Asia, leading to enhanced aeolian deposition and supply of material to the Baode region, as well as deposition in the Baode Paleolake through slope erosion and transportation by flowing water.

Comparing LZG9 to LZG11, it is evident that LZG9 exhibits higher peaks at ~200 Ma and ~1800 Ma. This coincides with the Miocene–Pliocene transition and the shift from Baode Red Clay to Jingle Red Clay deposition in the Baode area (Zhu et al., 2008). The significantly wetter climatic conditions during this period led to increased surface runoff (Ao et al., 2021), enhanced local erosion capacity, and a greater contribution of materials from the East Mu Us (EMU) desert and the Lüliang Mountains. Samples LZG8 and LZG6 both reflect a similar provenance, characterized by a mixture of materials originating from the Lüliang Mountains and EMU, in alignment with the sediment composition found on the planation surface of the Hequ section.

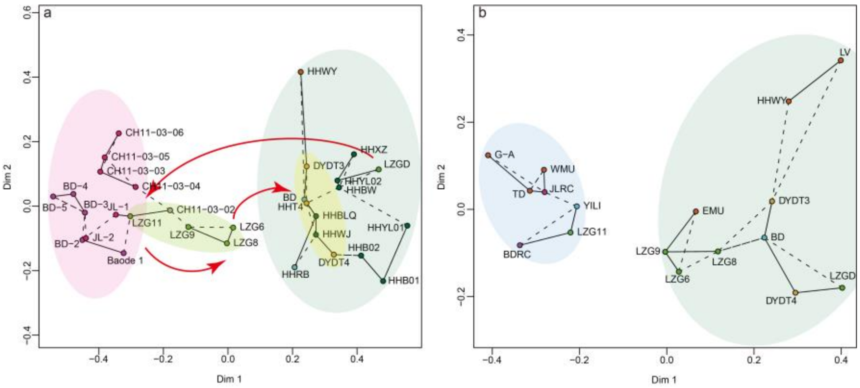

Figure 6. Non-matrix multi-dimensional scaling (MDS) plot of U–Pb zircon-age data. The proximity between samples reflects their degree of similarity, with solid lines connecting them denoting the first level of similarity, while dashed lines represent the second level of similarity. Colored areas represent main potential sources (Red=Red Clay, Green=Lüliang mountains and Ordos Block, Pale Green=Luzigou section, Yellow=Yellow River terraces, Blue=Central Asian Orogenic Belt and Tibetan Plateau) a.) Sediment similarity relationship between the Baode and Hequ regions. b.) The similarity of samples to potential source regions.

Incorporating MDS plots, our findings reveal two significant changes in provenance within the Luzigou section during the peneplanation period (Fig. 6). The first change occurred after the initial accumulation of fluvial gravel, whereas the second occurred before the formation of the G2 gravel unit at ~4.9 Ma. The basal gravel unit of the Luzigou fluvio-lacustrine strata signifies an inland water system characterized by a relatively simple provenance. However, due to the fine grain size of the lacustrine clay above the basal gravel unit, conducting zircon U–Pb chronology becomes challenging. Consequently, it proves difficult to determine the duration of the single provenance process and how the source evolved before 7.1 Ma, after which a change in provenance occurred prior to 4.9 Ma, which we attribute to intensified erosion resulting from increased climatic humidity (Ao et al., 2021). Enhanced runoff due to climatic humidity may have brought in more detrital, replacing a pattern dominated by aeolian deposition. Concurrently, we can discount additional provenance changes in the local area resulting from potential alterations in the source of the Red Clay. Within the Baode region, variation in the source of Baode Red Clay and Jingle Red Clay during this period is comparatively minor compared to fluctuations observed in the fluvio-lacustrine sediments (Shang et al., 2016; Bohm et al., 2023) and is thus inadequate as an explanation of provenance variation within the Luzigou section. In contrast, the analysis of Red Clay provenance in the Jiaxian section may offer greater insights into the formation of the north-flowing fluvio-lacustrine system of the Baode paleolake and its role in supplying weathered materials to the downwind Red Clay deposits (W.B. Peng et al., 2023).

Furthermore, previous studies suggest continuous and sequential accumulation of aeolian sediments in the Baode area, extending back to at least 7.1 Ma (Zhu et al., 2008), sediments that probably represented a consistent supply of material to the Baode Paleolake. The observed changes in sediment provenance can be attributed to increased contributions of silt- to sand-size detritus from local rivers. It is important to note that the zircon U–Pb method exhibits greater sensitivity to this grain size, owing to inherent limitations of the technique itself. Consequently, the influx of fluvial material gradually replaced the previously eroded local Red Clay, assuming a dominant role within the sedimentary record of the Baode Paleolake.

6.2 Provenance of sediments of the integrated Yellow River

The sediment provenance of the modern Yellow River bedload gravel has been a subject of significant interest and investigation among geologists due to the discovery that provenance may exhibit spatial variability across different sections of the river (Kong et al., 2014; Nie et al., 2015). In these studies, there has been focus on the Hetao Basin to Baode region, located around the northern part of the Jinshaan Gorge, where notable provenance variations have been observed, as exemplified by samples YILI and BD of Nie et al. (2015). Furthermore, the sediment provenance in the Yumenkou area at the southern end of the Jinshaan Gorge shares similarities with the BD samples, indicating a local source from the Ordos Block and the adjacent Lüliang Mountains (Kong et al., 2014). These findings suggest that the contemporary processes governing sediment transport in the middle reaches of the Yellow River system impede the passage of materials originating from the Tibetan Plateau through the Jinshaan Gorge. Consequently, these materials fail to reach downstream regions such as the North China Plain or the Bohai Sea. This observation highlights the complex dynamics of sediment transport and underscores the need for a comprehensive understanding of sediment provenance across different sections of the Yellow River system.

The investigation of zircon-age spectrums in the terrace gravels of the Hequ section has yielded crucial insights into the temporal extent of the sediment transport process, suggesting a possible duration from the terrace HHT4 formed (0.1 Ma) to present (Xiong et al., 2022). Notably, the analysis of samples DYDT4 and DYDT3 in this study, in combination with data from previously published samples YILI, BD, HHRB, and HHT4, reveals that material sourced from the upper reaches of the Hetao ~~basin~~ Basin has been impeded in reaching the Baode area since the initial formation of the integrated Yellow River. This timeframe pre-dates the formation of the highest Yellow River terrace, estimated at 1.2 Ma, based on previous paleomagnetic chronostratigraphy

(Pan et al., 2012). These findings suggest that the disruption in sediment transport from the upstream Hetao ~~basin~~ Basin to the Baode area occurred prior to the formation of the highest terrace, indicating prolonged restriction in sediment transport during this earlier period.

6.3 Drainage reorganization along the Jinshaan Gorge recorded by the provenance change

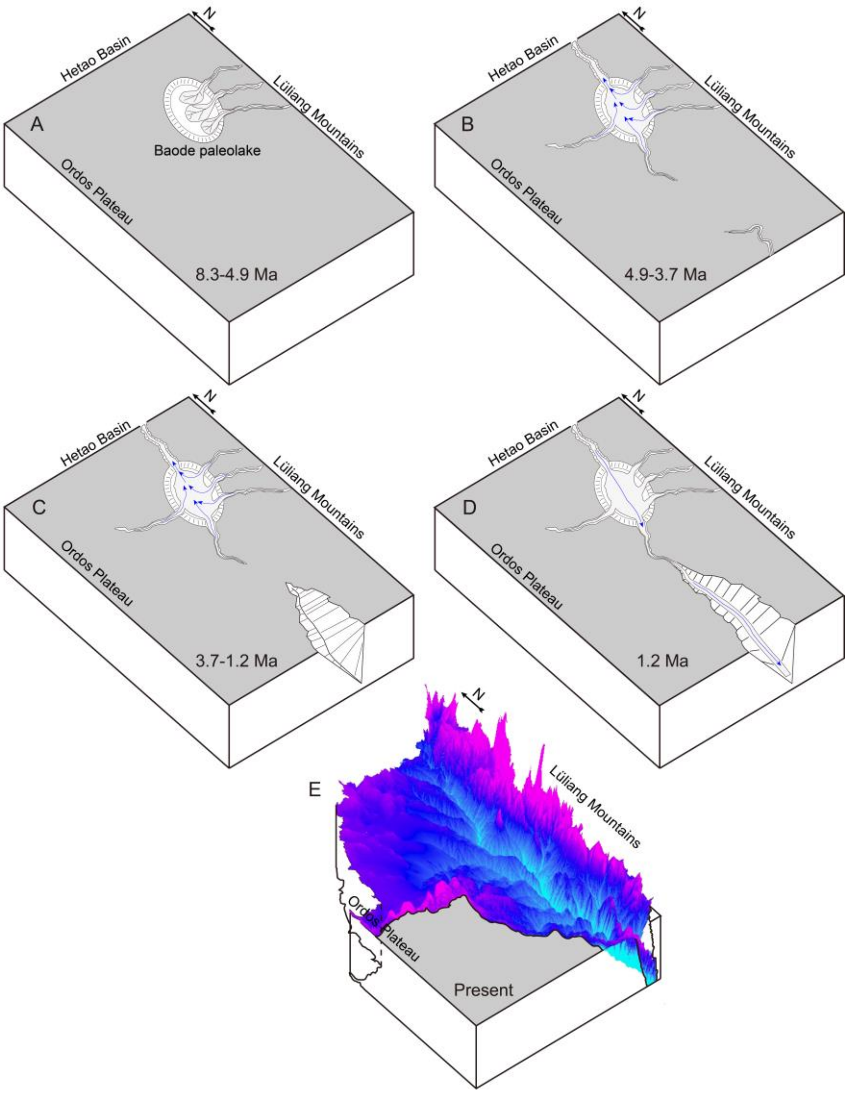

Figure 7. Time-slice sketch of evolutionary model in the northern Jinshaan Gorge since the Late-Miocene.

Our study has revealed noteworthy distinctions in provenance between the fluvio-lacustrine (LZG8 and LZG6) and terrace samples (DYDT4, DYDT3, and HHT4). Although the visual disparity on the KDE plots may not be obvious, a significant increase in the ~1800 Ma peak introduces a distinct separation between these two datasets on the MDS plots (Fig. 6). This disparity in provenance can be attributed to the intensified hydrodynamics following the formation of the integrated Yellow River, in which the reworking of Red Clay into fluvial deposits became limited. In contrast, the terrace samples exhibit a simpler local source that aligns with the characteristics of modern riverbed samples.

In this study, we present a comprehensive model for drainage evolution in the northern section of the Jinshaan Gorge, as illustrated in Figure 7. During the peneplanation period, from 8.3 to 4.9 Ma, a depression existed in the Baode area, resulting in the deposition of fluvio-lacustrine strata in the Baode paleolake, the main sediment source being the Red Clay. At 4.9 Ma, continued increasing of climatic humidity led either to the overflow of the lake or an inland river flowing into the Hetao ~~basin~~ Basin eroded headward and incised through the paleolake, giving rise to a paleo-river that flowed in the opposite direction to the modern Yellow River. Subsequently, at 3.7 Ma, the dissection of the ~~Tangxian~~ Tangxian-period planation surface triggered increased fluvial erosion, so that rivers originating from the Fenwei Basin began to erode northward along the western piedmont of the Lüliang Mountains as the headward erosion pattern in Hu et al. (2016). This pattern of headward erosion is similar to that proposed by the previous study in Sanmen Gorge (Liang et al., 2022). And the erosion process persisted until 1.2 Ma, when there was finally fluvial incision through the Baode area, resulting in the formation of the modern Yellow River. Concurrently, the initiation of the Jinshaan Gorge occurred, followed by the progressive incision that led to the formation of the Yellow River terrace sequence.

In conclusion, we emphasize that the formation of the modern configuration of the Yellow River in the Jinshaan Gorge occurred between 3.7 Ma and 1.2 Ma, following the dissection of the planation surface and preceding the formation of the highest terrace. Varied interpretations of the remaining sediments within the gorge have resulted in divergent views on the timing of Yellow River formation in previous studies ~~(Pan et al., 2011; Liu et al., 2020; Li et al., 2022; Xiong et al., 2022)~~. One of the viewpoints suggests that the fluvio-lacustrine~~remaining~~ sediments overlying the~~of~~ planation surface can probably be interpreted as~~represent~~ the archive~~deposits~~ of ancient Yellow River, excavating~~shaping~~ a wide valley by lateral erosion through the whole Jinshaan Gorge~~, and implies a steady river system~~ in the period from~~during~~ 8 to ~~–~~3.7 Ma ~~from Hetao Basin to Fenwei Basin~~ (Liu, 2020; Li et al., 2022; Xiong et al., 2022). In contrast, more evidences from terrace correlation and lithological composition argue an independent origination between the fluvio-lacustrine sediments accumulated on planation surface and the Yellow River terraces~~The other suggests the ancient river during peneplanation period is uncomparable with modern Yellow River, and the formation of highest terrace represents the Yellow River formed~~ (Cheng et al., 2002; Pan et al., 2012~~1~~; Hu et al., 2016, 2017, 2019). The ~~This~~ comprehensive provenance study here seems to be correspondent to the latter~~strongly supports the second view~~, conclud~~show~~ing that the fluvio-lacustrine deposits on the Tangxian-period planation surface~~within the Jinshaan Gorge~~~~These deposits~~ probably represent distinct endorheic drainage system during peneplain~~different stages of planation surface~~ development across the northern Jinshaan Gorge, rather than being attributable to

Formatted: Not Highlight

the modern integrated Yellow River. First, their distribution lacks connectivity and is difficult to relate to other parts of the Jinshaan Gorge area parallel to the Yellow River. Second, comprehensive provenance evidence in support of their association with more modern Yellow River deposits is lacking. While our study focuses primarily on the provenance differences between sediments overlying the planation surface and those of the modern Yellow River in the northern part of the Jinshaan Gorge, further investigations encompassing the entire gorge are clearly warranted. Nonetheless, it is evident that the presence of the Yellow River in the northern segment of the Jinshaan Gorge postdates 3.7 Ma.

We also would like to highlight an interesting observation regarding the headward erosion of the Yellow River during the period from 3.7 to 1.2 Ma. Our analysis reveals a distance of headward erosion during this period of ~410 km, at an average rate of 164 km/Ma (Hu et al., 2016). It is important to note that this erosion rate is significantly less than the headward-erosion rate of 350 km/Ma calculated by Craddock et al. (2010) for the Yellow River in the northeastern Tibetan Plateau. This discrepancy may be attributed to the different tectonic backgrounds of the two regions, with more active tectonic uplift in the northeastern Tibetan Plateau. ~~In addition~~Furthermore~~, during the Plio-Pleistocene,~~ numerous ~~significant global~~ drainage reorganization archives originated from the global view~~events~~ all appear to occur~~red~~ in the Plio-Pleistocene period (Gouveia et al., 2020; Yang et al., 2021), yielding a remarkable correlation~~closely associated~~ with the worldwide warming and wett~~humid~~ing climate ~~of that period~~ (Nie et al., 2014; Freitas et al., 2022). The process of drainage reorganization can vary based on the specific tectonic, climatic, and geomorphological settings, emphasizing the need to consider these factors holistically when reconstructing evolutionary history. Incorporating these elements into the analysis will contribute to a more comprehensive understanding of the complex reorganization processes associated with drainage in different regions.

7. Conclusions

Taking into consideration the spatial distribution of geomorphic surfaces, sedimentary characteristics, and provenance analysis, we have reconstructed the evolutionary history of the northern section of the Jinshaan Gorge from the peneplanation period to the development of the modern deeply incised valley of the Yellow River. Our investigation encompasses Late Miocene to Early Pleistocene time, capturing key provenance changes within this timeframe. The Baode paleolake emerged around 8.3 Ma as a localized endorheic system. Subsequently, at ~4.9 Ma, it became established as a fluvio-lacustrine system in conjunction with the Hetao Basin, resulting in northward outflow. As this process continued, the enhanced erosion resulting from the formation of the planation surface at ~3.7 Ma further reshaped the landscape. Finally, at 1.2 Ma, the downstream river captured the fluvio-lacustrine system, forming the present-day Yellow River middle reaches. Our study provides a robust framework that offers a comprehensive and reliable explanation for the evolution of the middle Yellow River catchment, taking into account the significant influences of increasing climatic humidity and relative tectonic uplift.

Acknowledgments

This article is dedicated to the memory of Prof. Rob W.C. Westaway, a distinguished geologist and geomorphologist. We thank Prof. Martin Gibling for reviewing and improving the initial version of this manuscript~~, which improved the paper significantly~~. This research was financially supported by the National Natural Science Foundation of China (Grant no. 42041006; Grant no. ~~41871001~~42371001), the Fundamental Research Funds for the Central Universities, China (lzujbky-2022-ey10), and 111 Program from State Administration of Foreign Experts Affairs and Ministry of Education of the People's Republic of China (Grant no. BP2018001). ~~This article is honourably dedicated to our lifelong friend, Rob Westaway.~~

References

Ao, H., Rohling, E.J., Zhang, R., Roberts, A.P., Holbourn, A.E., Ladant, J.B., Dupont-Nivet, G., Kuhnt, W., Zhang, P., Wu, F., Dekkers, M.J., Liu, Q.S., Liu, Z.H., Xu, Y., Poulsen, C.J., Licht, A., Sun, Q., Chiang, O., Liu, X.D., Wu, G.X., Ma, C., Zhou, W.J., Jin, Z.D., Li, X.X., Li, X.Z., Peng, X.Z., Qiang, X.K., An, Z.S., 2021. Global warming-induced Asian hydrological climate transition across the Miocene-Pliocene boundary. Nat. Commun., 12(1). https://doi.org/10.1038/s41467-021-27054-5.

Bar, O., Zilberman, E., Feinstein, S., Calvo, R., Gvirtzman, Z., 2016. The uplift history of the Arabian Plateau as inferred from geomorphologic analysis of its northwestern edge. Tectonophysics, 671, 9-23. https://doi.org/10.1016/j.tecto.2016.01.004.

Bohm, K., Kaakinen, A., Stevens, T., Lahaye, Y., Tang, H., Shang, Y., Zhang, H.Z., Lu, H.Y., 2023. Neogene global climate change and East Asian dust sources: Combined rutile geochemistry and zircon U-Pb analysis from the northern Chinese Loess Plateau. Global Planet Change, 221, 104049. https://doi.org/10.1016/j.gloplacha.2023.104049.

Cheng, S.P., Deng, Q.D., Zhou, S.W., Yang, G.Z., 2002. Strath terraces of Jinshaan Canyon, Yellow River, and Quaternary tectonic movements of the Ordos Plateau, North China. Terra Nova, 14(4), 215-224. https://doi.org/10.1046/j.1365-3121.2002.00350.x.

Craddock, W.H., Kirby, E., Harkins, N.W., Zhang, H.P., Shi, X.H., Liu, J.H., 2010. Rapid fluvial incision along the Yellow River during headward basin integration. Nat. Geosci., 3(3), 209-213. https://doi.org/10.1038/ngeo777.

Davis, W.M., 1899. The geographical cycle. Geographical J., 14(5),481–504. http://www.jstor.org/stable/1774538.

Evenstar, L.A., Hartley, A.J., Stuart, F.M., Mather, A.E., Rice, C.M., Chong, G., 2009. Multiphase development of the Atacama Planation Surface recorded by cosmogenic He-3 exposure ages: Implications for uplift and Cenozoic climate change in western South America. Geology, 37(7), 658-658. https://doi.org/10.1130/G25437A.1.

Freitas, M.M.d., Paixão, R.W., Salgado, A.A.R., Eirado Silva, L.G., Cunha, P.P., Gomes, A.A.T., Martins, A.A., Almeida, J.C.H., Tupinambá, M.A., Dantas, M., 2022. The endorheic – Exorheic transition and later stage of fluvial incision in a wet tropical margin setting: The Atlantic draining Paraíba do Sul River basin (Brazil). Journal of South American Earth Sciences, 115, 103742. https://doi.org/10.1016/j.jsames.2022.103742.

Gouveia, M.P., Cunha, P.P., Falguères, C., Voinchet, P., Martins, A.A., Bahain, J.-J., Pereira, A., 2020. Electron spin resonance dating of the culminant allostratigraphic unit of the Mondego and Lower Tejo Cenozoic basins (W Iberia), which predates fluvial incision into the basin-fill sediments. Global Planet Change, 184, 103081. https://doi.org/10.1016/j.gloplacha.2019.103081

Guillocheau, F., Simon, B., Baby, G., Bessin, P., Robin, C., Dauteuil, O., 2018. Planation surfaces as a record of mantle dynamics: The case example of Africa. Gondwana Res., 53, 82-98.

https://doi.org/10.1016/j.gr.2017.05.015.

Hu, Z.B., Li, M.H., Dong, Z.J., Guo, L.Y., Bridgland, D., Pan, B.T., Li, X.H., Liu, X.F., 2019. Fluvial entrenchment and integration of the Sanmen Gorge, the Lower Yellow River. Global Planet Change, 178, 129-138. https://doi.org/10.1016/j.gloplacha.2019.04.010.

Hu, Z.B., Pan, B.T., Bridgland, D., Vandenberghe, J., Guo, L.Y., Fan, Y.L., Westaway, R., 2017. The linking of the upper-middle and lower reaches of the Yellow River as a result of fluvial entrenchment. Quaternary Sci. Rev., 166, 324-338. https://doi.org/10.1016/j.quascirev.2017.02.026.

Hu, Z.B., Pan, B.T., Guo, L.Y., Vandenberghe, J., Liu, X.P., Wang, J.P., Fan, Y.L., Mao, J.W., Gao, H.S., Hu, X.F., 2016. Rapid fluvial incision and headward erosion by the Yellow River along the Jinshaan gorge during the past 1.2 Ma as a result of tectonic extension. Quaternary Sci. Rev., 133, 1-14. https://doi.org/10.1016/j.quascirev.2015.12.003.

Huang, X., Wang, Y.N., Zhang, J., Wu, F.Z., Yang, Y.L., 2022. Low-temperature thermochronological insights into the Mesozoic-Cenozoic exhumation history of the Taihang-Lvliangshan region: A review. Geological Journal, 57(4), 1511-1529. https://doi.org/10.1002/gj.4352.

Jackson, S.E., Pearson, N.J., Griffin, W.L., Belousova, E.A., 2004. The application of laser ablation-inductively coupled plasma-mass spectrometry to in situ U-Pb zircon geochronology. Chem. Geol., 211(1-2), 47-69. https://doi.org/10.1016/j.chemgeo.2004.06.017.

King, L.C., 1953. Canons of landscape evolution. Geol. Soc. Am. Bull., 64, 721-752. https://doi.org/10.1130/0016-7606(1953)64[721:COLE]2.0.CO;2.

Kong, P., Jia, J., Zheng, Y., 2014. Time constraints for the Yellow River traversing the Sanmen

Gorge. Geochem. Geophys. Geosyst., 15(2), 395-407. https://doi.org/10.1002/2013GC004912.

Li, J.J., 1991. The Environmental-Effects of the Uplift of the Qinghai-Xizang Plateau. Quaternary Sci. Rev., 10(6), 479-483. https://doi.org/10.1016/0277-3791(91)90041-R.

Li, J.J., 1999. In memory of Davisian Theory of erosion cycle and peneplain：a centurial study in China. Journal of Lanzhou University (Natural Sciences), 35(3), 157-163. https://doi.org/10.13885/j.issn.0455-2059.1999.03.018. (in Chinese, with English abstract)

Li, J.X., 2009. Discovery and geological significance of red clay in the Liulin section in the west part of Lvliang Mountains. ACTA Sedimentologica Sinica, 27(6), 1184-1190. https://doi.org/10.14027/j.cnki.cjxb.2009.06.017. (in Chinese, with English abstract)

Li, X.H., Liu, Y., Li, Q.L., Guo, C.H., Chamberlain, K.R., 2009. Precise determination of Phanerozoic zircon Pb/Pb age by multicollector SIMS without external standardization. Geochem. Geophys. Geosyst., 10. https://doi.org/10.1029/2009GC002400.

Li, Z.Y., Zhang, K., Liang, H., Chen, Z., Ma, Z.W., Xiong, J.G., Huang, P., 2022. Large river chronology along the Jinshaan Gorge on the Yellow River and its implications for initialization. Geomorphology, 400. https://doi.org/10.1016/j.geomorph.2021.108092.

Liang, H., Zhang, K., Li, Z., Fu, J., Yu, Z., Xiong, J., Li, X., Ma, Z., Huang, P., Li, Z., Zhang, Y., Hui, G., Tian, Q., Wang, W., Zheng, W., Zhang, P., 2022. How headward erosion breaches upstream paleolakes: Insights from dated longitudinal fluvial terrace correlations within the Sanmen Gorge, Yellow River. GSA Bulletin, 135(5-6), 1602-1617. https://doi.org/10.1130/B36537.1.

Licht, A., Dupont-Nivet, G., Pullen, A., Kapp, P., Abels, H.A., Lai, Z., Guo, Z., Abell, J., Giesler, D., 2016. Resilience of the Asian atmospheric circulation shown by Paleogene dust provenance. Nat. Commun., 7. https://doi.org/10.1038/ncomms12390.

Liu, C.H., Zhao, G.C., Sun, M., Zhang, J., He, Y.H., Yin, C.Q., Wu, F.Y., Yang, J.H., 2011. U-Pb and Hf isotopic study of detrital zircons from the Hutuo group in the Trans-North China Orogen and tectonic implications. Gondwana Res., 20(1), 106-121. https://doi.org/10.1016/j.gr.2010.11.016.

Liu, Q.S., Jin, C.S., Hu, P.X., Jiang, Z.X., Ge, K.P., Roberts, A.P., 2015. Magnetostratigraphy of Chinese loess-paleosol sequences. Earth-Sci. Rev., 150, 139-167. https://doi.org/10.1016/j.earscirev.2015.07.009.

Liu, S.W., Zhang, J., Li, Q.G., Zhang, L.F., Wang, W., Yang, P.T., 2012. Geochemistry and U-Pb zircon ages of metamorphic volcanic rocks of the Paleoproterozoic Luliang Complex and constraints on the evolution of the Trans-North China Orogen, North China Craton. Precambrian Res., 222, 173-190. https://doi.org/10.1016/j.precamres.2011.07.006.

Liu, Y.M., 2020. Neogene fluvial sediments in the northern Jinshaan Gorge, China: Implications for early development of the Yellow River since 8 Ma and its response to rapid subsidence of the Weihe-Shanxi Graben. Palaeogeogr. Palaeoclimatol. Palaeoecol., 546. https://doi.org/10.1016/j.palaeo.2020.109675.

Lu, H.Y., Zhang, H.Z., Feng, H., Wang, Y.C., Cai, D.X., Li, G.W., Lyu, H., Lei, F., Wang, K.X., Wang, S.M., Lai, W., Wang, X.Y., 2023. Landform evolution in Asia during the Cenozoic revealed by formation of drainages of Wei River and Indus River. Palaeogeogr. Palaeoclimatol. Palaeoecol., 619. https://doi.org/10.1016/j.palaeo.2023.111516.

Miao, X.D., Lu, H.Y., Li, Z., Cao, G.C., 2008. Paleocurrent and fabric analyses of the imbricated fluvial gravel deposits in Huangshui Valley, the northeastern Tibetan Plateau, China. Geomorphology, 99(1-4), 433-442. https://doi.org/10.1016/j.geomorph.2007.12.005.

Nie, J.S., Stevens, T., Rittner, M., Stockli, D., Garzanti, E., Limonta, M., Bird, A., Ando, S., Vermeesch, P., Saylor, J., Lu, H.Y., Breecker, D., Hu, X.F., Liu, S.P., Resentini, A., Vezzoli, G., Peng, W.B., Carter, A., Ji, S.C., Pan, B.T., 2015. Loess Plateau storage of Northeastern Tibetan Plateau-derived Yellow River sediment. Nat. Commun., 6. https://doi.org/10.1038/ncomms9511.

Nie, J.S., Zhang, R., Necula, C., Heslop, D., Liu, Q.S., Gong, L.S., Banerjee, S., 2014. Late Miocene- early Pleistocene paleoclimate history of the Chinese Loess Plateau revealed by remanence unmixing. Geophys Res Lett, 41(6), 2163-2168. https://doi.org/10.1002/2014GL059379.

Orme, A.R., 2013. 1.12 Denudation, planation, and cyclicity: myths, models, and reality. Treatise on Geomorphology, 1, 205-232. https://doi.org/10.1016/B978-0-12-374739-6.00012-9.

Pan, B.T., Hu, Z.B., Wang, J.P., Vandenberghe, J., Hu, X.F., 2011. A magnetostratigraphic record of landscape development in the eastern Ordos Plateau, China: Transition from Late Miocene and Early Pliocene stacked sedimentation to Late Pliocene and Quaternary uplift and incision by the Yellow River. Geomorphology, 125(1), 225-238. https://doi.org/10.1016/j.geomorph.2010.09.019.

Pan, B.T., Hu, Z.B., Wang, J.P., Vandenberghe, J., Hu, X.F., Wen, Y.H., Li, Q., Cao, B., 2012. The approximate age of the planation surface and the incision of the Yellow River. Palaeogeogr. Palaeoclimatol. Palaeoecol., 356, 54-61. https://doi.org/10.1016/j.palaeo.2010.04.011.

Formatted: Default Paragraph Font, Font: (Default) +Body (DengXian)

Peng, H., Wang, J.Q., Liu, C.Y., Zhao, H.G., Huang, L., Zhao, X.C., Zhang, S.H., Liang, C., Wang, Z., Jiao, X.Q., Zhang, L., Zhang, T.B., Zhang, D.D., Zattin, M., Catto, S., 2023. Long-term and multiple stage exhumation of the Ordos Basin, western North China Craton: Insights from seismic reflection, borehole and geochronological data. Earth-Sci. Rev., 238. https://doi.org/10.1016/j.earscirev.2023.104349.

Peng, W.B., Nie, J.S., Wang, Z., Qiang, X.K., Garzanti, E., Pfaff, K., Song, Y.G., Stevens, T., 2018. A major change in precipitation gradient on the Chinese Loess Plateau at the Pliocene-Quaternary boundary. J. Asian Earth Sci., 155, 134-138. https://doi.org/10.1016/j.jseaes.2017.10.031.

Peng, W.B., Zhang, H.B., Pullen, A., Li, M.T., Pan, B.T., Xiao, W.J., Nie, J.S., 2023. Stepwise increased spatial provenance contrast on the Chinese Loess Plateau over late Miocene-Pleistocene. Commun. Earth Environ., 4(1). https://doi.org/10.1038/s43247-023-00721-9.

Shang, Y., Beets, C.J., Tang, H., Prins, M.A., Lahaye, Y., van Elsas, R., Sukselainen, L., Kaakinen, A., 2016. Variations in the provenance of the late Neogene Red Clay deposits in northern China. Earth Planet. Sci. Lett., 439, 88-100. https://doi.org/10.1016/j.epsl.2016.01.031.

Shi, W., Dong, S.W., Hu, J.M., 2020. Neotectonics around the Ordos Block, North China: A review and new insights. Earth-Sci. Rev., 200. https://doi.org/10.1016/j.earscirev.2019.102969.

Slama, J., Kosler, J., Condon, D.J., Crowley, J.L., Gerdes, A., Hanchar, J.M., Horstwood, M.S.A., Morris, G.A., Nasdala, L., Norberg, N., Schaltegger, U., Schoene, B., Tubrett, M.N., Whitehouse, M.J., 2008. Plesovice zircon - A new natural reference material for U-Pb and Hf isotopic microanalysis. Chem. Geol., 249(1-2), 1-35. https://doi.org/10.1016/j.chemgeo.2007.11.005.

Souza, D.H., Parra, M., del Rio, I., Sawakuchi, A.O., Pupim, F.N., Hernandez-Gonzalez, J.S., Gomez, S., 2022. Late Quaternary Drainage Rearrangement Prevents the Vegetation Development in the La Tatacoa Intermontane Basin of the Colombian Andes. Front Earth Sc-Switz, 10. https://doi.org/10.3389/feart.2022.808718.

Stevens, T., Carter, A., Watson, T.P., Vermeesch, P., Ando, S., Bird, A.F., Lu, H., Garzanti, E., Cottam, M.A., Sevastjanova, I., 2013. Genetic linkage between the Yellow River, the Mu Us desert and the Chinese Loess Plateau. Quaternary Sci. Rev., 78, 355-368. https://doi.org/10.1016/j.quascirev.2012.11.032.

Stevens, T., Palk, C., Carter, A., Lu, H.Y., Clift, P.D., 2010. Assessing the provenance of loess and desert sediments in northern China using U-Pb dating and morphology of detrital zircons. Geol. Soc. Am. Bull., 122(7-8), 1331-1344. https://doi.org/10.1130/B30102.1.

Strahler, A.N., 1950. Davis' concepts of slope development viewed in the light of recent quantitative investigations. Annals of the Association of American Geographers, 40(3), 209–213. https://doi.org/10.1080/00045605009352069.

Sun, J.M., Ding, Z.L., Xiao, W.J., Windley, B.F., 2022. Coupling between uplift of the Central Asian Orogenic Belt-NE Tibetan Plateau and accumulation of aeolian Red Clay in the inner Asia began at-7 Ma. Earth-Sci. Rev., 226. https://doi.org/10.1016/j.earscirev.2022.103919.

Vermeesch, P., 2012. On the visualisation of detrital age distributions. Chem. Geol., 312, 190-194. https://doi.org/10.1016/j.chemgeo.2012.04.021.

Vermeesch, P., 2013. Multi-sample comparison of detrital age distributions. Chem. Geol., 341, 140-146. https://doi.org/10.1016/j.chemgeo.2013.01.010.

Wang, X., Zhu, W.B., Ge, R.F., Luo, M., Zhu, X.Q., Zhang, Q.L., Wang, L.S., Ren, X.M., 2014.

Two episodes of Paleoproterozoic metamorphosed mafic dykes in the Lvliang Complex: Implications for the evolution of the Trans-North China Orogen. Precambrian Res., 243, 133-148. https://doi.org/10.1016/j.precamres.2013.12.014.

Wiedenbeck, M., Alle, P., Corfu, F., Griffin, W.L., Meier, M., Oberli, F., Vonquadt, A., Roddick, J.C., Speigel, W., 1995. 3 Natural Zircon Standards for U-Th-Pb, Lu-Hf, Trace-Element and Ree Analyses. Geostandard Newslett., 19(1), 1-23. https://doi.org/10.1111/j.1751-908X.1995.tb00147.x.

Woolfe, K.J., Stewart, L.K., Francis, J.E., Arnot, M.J., 2000. PC99: a new freeware for manipulating and graphically displaying palaeocurrent data. Sediment Geol., 133(1-2), 1-5. https://doi.org/10.1016/S0037-0738(00)00034-8.

Xiao, G.Q., Sun, Y.Q., Yang, J.L., Yin, Q.Z., Dupont-Nivet, G., Licht, A., Kehew, A.E., Hu, Y.Z., Geng, J.Z., Dai, G.W., Zhao, Q.Y., Wu, Z.P., 2020. Early Pleistocene integration of the Yellow River I: Detrital-zircon evidence from the North China Plain. Palaeogeogr. Palaeoclimatol. Palaeoecol., 546, 0031-0182. https://doi.org/10.1016/j.palaeo.2020.109691.

Xiong, J.G., Li, Y.L., Zheng, W.J., Zhang, P.Z., Lei, J.H., Zhong, Y.Z., Hu, X., Li, Z.G., Gong, Z., Li, T., Zhang, Y.P., Xu, B.B., Tian, Q.Y., Xin, W.L., Ren, X.L., Yao, Y.F., 2018. Climatically driven formation of the Tangxian planation surface in North China: An example from northwestern Zhongtiao Shan of the Shanxi Graben System. Lithosphere, 10(4), 530-544. https://doi.org/10.1130/L720.1.

Xiong, J.G., Liu, Y.M., Zhang, P.Z., Deng, C.L., Picotti, V., Wang, W.T., Zhang, K., Liang, H., Zhao, X.D., Zhong, Y.Z., Liu, Q.R., Lei, J.H., Kang, H., Ren, Z.K., Zhang, H.P., Li, Y.L., 2022.

Entrenchment of the Yellow River since the late Miocene under changing tectonics and climate. Geomorphology, 416. https://doi.org/10.1016/j.geomorph.2022.108428.

Xu, Y., Yue, L.P., Li, J.X., Sun, L., Sun, B., Zhang, J.Y., Ma, J., Wang, J.Q., 2009. An 11-Ma-old red clay sequence on the Eastern Chinese Loess Plateau. Palaeogeogr. Palaeoclimatol. Palaeoecol., 284(3-4), 383-391. https://doi.org/10.1016/j.palaeo.2009.10.023.

Yang, J., Nie, J.S., Garzanti, E., Limonta, M., Andò, S., Vermeesch, P., Zhang, H.B., Hu, X.F., Wang, Z., Zhao, B.J., Ncube, L., Stevens, T., Li, M.T., Li, H., Chen, T.A., Miao, Y.F., Pan, B.T., 2021. Climatic Forcing of Plio- Pleistocene Formation of the Modern Limpopo River, South Africa. Geophys Res Lett, 48(14), e2021GL093887. https://doi.org/10.1029/2021GL093887.

Yue, L.P., Li, J.X., Zheng, G.Z., Li, Z.P., 2007. Evolution of the Ordos Plateau and environmental effects. Sci. China Ser. D., 50, 19-26. https://doi.org/10.1007/s11430-007-6013-2.

Zhang, H.Z., Lu, H.Y., Xu, X.S., Liu, X.M., Yang, T., Stevens, T., Bird, A., Xu, Z.W., Zhang, T., Lei, F., Feng, H., 2016. Quantitative estimation of the contribution of dust sources to Chinese loess using detrital zircon U-Pb age patterns. J. Geophys. Res. Earth Surf., 121(11), 2085-2099. https://doi.org/10.1002/2016JF003936.

Zhang, H.Z., Lu, H.Y., Zhou, Y.L., Cui, Y.Y., He, J., Lv, H.Z., Wang, K.X., Wang, X.Y., 2021. Heavy mineral assemblages and U-Pb detrital zircon geochronology of sediments from the Weihe and Sanmen Basins: New insights into the Pliocene-Pleistocene evolution of the Yellow River. Palaeogeogr. Palaeoclimatol. Palaeoecol., 562. https://doi.org/10.1016/j.palaeo.2020.110072.

Zhang, R., Nie, J.S., 2017. Goethite Concentration Variations in the Red Clay Sequence on the

Formatted: Default Paragraph Font, Font: (Default) +Body (DengXian)

Chinese Loess Plateau. Geochem. Geophys. Geosyst., 18(11), 4179-4185. https://doi.org/10.1002/2017GC007148.

Zhao, G.C., Wilde, S.A., Sun, M., Li, S.Z., Li, X.P., Zhang, J., 2008. SHRIMP U-Pb zircon ages of granitoid rocks in the Luliang Complex: Implications for the accretion and evolution of the Trans-North China Orogen. Precambrian Res., 160(3-4), 213-226. https://doi.org/10.1016/j.precamres.2007.07.004.

Zhao, J.F., Liu, C.Y., Mountney, N., Lu, J.J., Cao, J.L., Yang, Y., Xue, R., 2016. Timing of uplift and evolution of the Luliang Mountains, North China Craton. Sci. China Earth Sci., 59(1), 58-69. https://doi.org/10.1007/s11430-015-5153-z.

Zhu, Y.M., Zhou, L.P., Mo, D.W., Kaakinen, A., Zhang, Z.Q., Fortelius, M., 2008. A new magnetostratigraphic framework for late Neogene Hipparion Red Clay in the eastern Loess Plateau of China. Palaeogeogr. Palaeoclimatol. Palaeoecol., 268(1-2), 47-57. https://doi.org/10.1016/j.palaeo.2008.08.001.

Plio-Pleistocene drainage reorganization in the middle Yellow River of China, revealed by provenance and paleocurrent analysis of fluvial sediments

Menghao Li[1], Zhenbo Hu[1,2,3*], Ping Wang[4*], Baotian Pan[1,2,3], David Bridgland[5], Qinhong Mo[1], Xiaohua Li[1], Zijuan Dong[1], Meiling Zhong[1], Renzhe Pan[1], Ningyi Li[1]

[1] Key Laboratory of Western China's Environmental Systems (Ministry of Education), College of Earth and Environmental Sciences, Lanzhou University, Lanzhou, 730000, China.

[2] Institute of Green Development for the Yellow River Drainage Basin, Lanzhou University, Lanzhou, 730000, China.

[3] Shiyang River Basin Scientific Observing Station of Gansu Province, Lanzhou, 730000, China.

[4] School of Geography, Nanjing Normal University, Nanjing, 210023, China.

[5] Department of Geography, Durham University, Lower Mountjoy, South Road, Durham DH1 3LE, United Kingdom of Great Britain and Northern Ireland

Corresponding author: Zhenbo Hu (zhbhu@lzu.edu.cn), Ping Wang (tigerwp@njnu.edu.cn)

Abstract

Continental-scale drainage reorganization is generally understood to result from landform evolution forced by the coupling between tectonic activity and climate change, attracting worldwide attention. Planation surfaces and river terraces constitute the most direct geomorphological archives for integrating the history of river systems and for reconstructing processes of drainage reorganization based on provenance analysis of the fluvial sediments. The Middle Yellow River has incised into the Ordos Block, which was previously levelled by a planation surface, creating the Jinshaan Gorge and linking the Hetao Basin to the north and the Fenwei Basin to the south. Multiple lines of evidence, from terraces correlation, sedimentary characteristics, and fluvial provenance, suggest that the Middle Yellow River catchment was occupied by fluvio-lacustrine systems before drainage integration, accumulating a sedimentary sequence derived from surrounding Red Clay and bedrocks during the period between 8.3 and 3.7 Ma. The planation surface was uplifted subsequently, forcing reorganization of the fluvio-lacustrine systems. Their integration resulted in the formation of the Jinshaan Gorge prior to 1.2 Ma. Numerous terraces were created during incision by the Middle Yellow River from north to south along the gorge. Our data, obtained from zircon U-Pb dating and lithological composition of fluvial gravels, further points to a remarkable discrepancy in provenance between the fluvio-lacustrine systems overlying the planation surface and the terraces sequence formed by the integrated Middle Yellow River, confirming the drainage reorganization process constrained by the geomorphic records.

1. Introduction

As a peneplain is regenerated by elevation into a new cycle of life, a planation surface initiates a renewed cycle of erosion (Davis, 1899), marking the replacement of pre-existing drainage systems by new deeply incised river valleys at lower levels. Following a century-long debate on the mechanisms that generate planation surfaces (Strahler, 1950; King, 1953; Orme, 2013), investigations conducted by geomorphologists have significantly advanced the understanding of geomorphic evolution and river development associated with planation events in recent decades (Evenstar et al., 2014; Bar et al., 2016; Guillocheau et al., 2018).

Numerous investigations have been undertaken to constrain the initiation of planation-surface dissection chronologically by analyzing the youngest stratigraphic layers incised by the planation surface and determining the age of the oldest overlying sediments (Pan et al., 2012; Bar et al., 2016; Xiong et al., 2018). These endeavors aim to establish a timeframe for the genesis of the landscapes observable presently. The extensively distributed Tangxian-period planation surfaces in China have emerged as a prominent subject of investigation within this field of research. The Tangxian-period planation surface extends along the western periphery of the North China Plain, stretching between the Taihang and Lüliang Mountains, and continues further onto the primary plateau surface of the Ordos Plateau (Pan et al., 2012; Hu et al., 2017; Xiong et al., 2018). Based on previous investigations, the formation of this planation surface probably commenced at 20 Ma, with sea level acting as the ultimate erosion base level (Li, 1999). The process involved weathering and erosion of the positive terrain, along with sedimentation filling the negative terrain, ultimately leading to the development of a peneplain-like landscape. The beginning of the dissection of the planation surface occurred at approximately 3.7 Ma as a consequence either of tectonic uplift or climate change, leading to the formation of the modern Yellow River and its tributaries (Li, 1991; Pan et al., 2011; Pan et al., 2012). However, the mechanisms and processes driving this landscape transformation remain debated.

The current scholarly deliberations revolve around two key aspects of this landscape history: first, the initial drainage pattern during the development of the peneplain before the formation of the Jinshaan Gorge section of the Yellow River and, second, the formation of the modern river system after the dissection of the planation surface. To address the above questions, considerable efforts have been devoted to the Tangxian-period planation surface and the downstream sedimentary basin (Pan et al., 2011, 2012; Hu et al., 2016; Xiong et al., 2018; Liu, 2020; Zhang et al., 2021; Li et al., 2022). Nevertheless, divergent interpretations arising from inconsistencies in materials or methods have led to a multitude of different patterns in drainage reorganization being hypothesized. To shed light on the process of drainage reorganization in the middle reaches of the Yellow River, this paper proposes an innovative approach that integrates comparative analysis of geomorphic surfaces and examination of the provenance of the overlying sediments.

This investigation focuses on the Baode section, a significant site extensively studied in relation to the Tangxian-period planation surface and the Neogene Red Clay in the middle reaches of the Yellow River (Zhu et al., 2008; Pan et al., 2011; Shang et al., 2016; Bohm et al., 2023). During the peneplanation period, the Baode region exhibited negative topography, with the surrounding endorheic drainage converging in a Baode paleolake (Pan et al., 2011). The center of lacustrine sediment accumulation was in the area of Luzigou, with a gradual decline in sediment thickness observed towards the lake edge. Simultaneously, the adjacent terrain experienced differential erosion, resulting in the removal of higher elevations and the deposition of Neogene aeolian Red Clay in areas that were comparatively lower and characterized by gentle slopes (Yue et al., 2007). The Neogene aeolian Red Clay divide into the Baode Red Clay (older than ~5.34 Ma) and Jingle

Red Clay at ~5.34 Ma (Zhu et al., 2008). Furthermore, remnants of gravel deposits are present on the planation surface, covered by Jingle Red Clay, and previous investigations have conjectured that these can be attributed to the endorheic drainage system during the peneplanation period (Pan et al., 2011, 2012). In terms of spatial distribution, these gravel units exhibit a parallel alignment with the Yellow River channel, extending across both sides of the modern valley. They resemble gravels associated with the Yellow River, but their lithological composition is relatively uncomplicated and distinct from these. In this study, we focus on the lithological composition and paleocurrents of these gravel units, comparing them with the sediments of the Baode paleolake and the Yellow River terraces, revealing a drainage system rerouted by a capture event. In addition, detrital zircon U–Pb chronology provenance studies of the Luzigou section and the Yellow River terraces have provided further information on the palaeo-hydrological pattern and evolutionary history of the Yellow River system.

2. Regional setting

2.1 General geology

The Ordos Block and the Lüliang Mountains are integral components of the North China Craton, comprising Archean and Paleoproterozoic metamorphic basement rocks that underwent reactivation and reconstruction during the Yanshanian orogeny (~137 Ma). The Ordos Block, formerly which was the Ordos Basin prior to the Cenozoic, was the scene of sediment accumulation from the Proterozoic to the Mesozoic (H. Peng et al., 2023). Exhumation and deformation occurred between the Eocene and the Late-Miocene, transforming the Ordos Block into a plateau. This was brought about by the northeastward growth of the Tibetan Plateau, which also led to the formation of initial faulted basins along the periphery of the Ordos Plateau (Shi et al., 2020). Following gradual uplift during the Yanshanian orogeny, the Lüliang Mountains were strongly uplifted during the Late Miocene (Zhao et al., 2016; Huang et al., 2021). Simultaneously, the faulted basins along the margins of the Ordos Plateau were further extended. These basins record sedimentary archives from the Eocene onwards and additionally serve as erosional base levels for the local drainage systems (Lu et al., 2023).

Starting in the Late Miocene, aeolian sediments have been deposited unconformably above the original landform, which may have suffered erosion by local fluvial or slope processes, with accumulation of residues in the lowlands (Yue et al., 2007). The deposition of Red Clay was initiated in the western piedmont of the Lüliang Mountains approximately 7 Ma, although differences in the age of its lower boundary are observed across multiple profiles, potentially associated with variations in the original landform (Xu et al., 2009; Ao et al., 2017; Sun et al., 2022). Between 3.7 and 2.6 Ma, typical aeolian sediments with a high mass magnetic susceptibility are present. Aeolian accumulation is linked to the overall uplift of the Tangxian-period peneplain and the complete isolation of some profiles from aqueous environments (Pan et al., 2011). In the Quaternary, a thick series of loess deposits accumulated continuously above the Red Clay, leading to the formation of the Chinese Loess Plateau, a prominent feature of the region's geological landscape (Liu et al., 2015).

2.2 Geographic setting

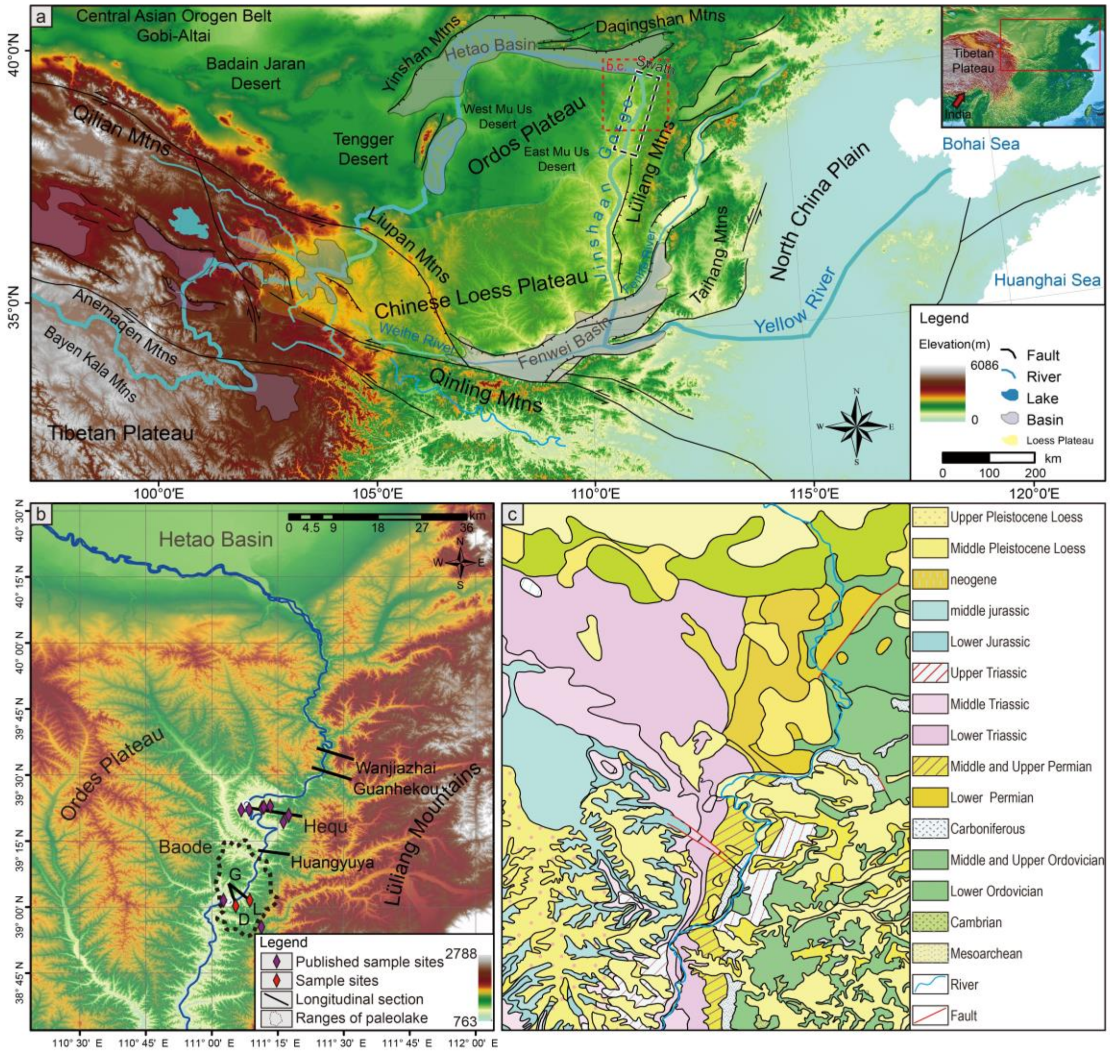

Figure 1. Topographic map, sampling sites, and geological map. a.) The Yellow River flows from the Tibetan Plateau, makes a U-shaped bend through the Hetao Basin, cuts through the Jinshaan Gorge, runs eastward across the Fenwei Basin, and finally reaches the North China Plain and flows into the Bohai Sea. b.) The longitudinal geomorphic sections and sampling sites studied for detrital zircon U–Pb dating in this and previous research are shown in different colors. (G: Gaojiayinze, D: Dayandun, L: Luzigou) c.) Stratigraphic units of varying geological epochs are delineated with different colors.

The present-day topography of the Ordos Plateau is characterized by higher elevations in the west and lower elevations in the east (Fig 1). At the western piedmont of the Lüliang Mountains, the elevation reaches approximately 1000 m. Originating from the northeastern Tibetan Plateau, the Yellow River follows a U-shaped bend within the Hetao Basin before flowing from north to south into the Fenwei Basin, passing through the western piedmont of the Lüliang Mountains. The section from the outlet of the Hetao Basin to the entrance of the Fenwei Basin is commonly referred to as the Jinshaan Gorge section of the Yellow River, which is notable for its deep valleys, high mountains, and rugged terrain. In conjunction with the deeply incised canyon, the Jinshaan Gorge encompasses several depressions that exhibit lower elevations compared to the Ordos Plateau, about 650~850 m. These depressions have facilitated the widening of the Yellow River valley and the development of local strath areas. Previous studies have speculated that these depressions might have been lakes during the peneplanation period, which were distributed sporadically along the Jinshaan Gorge and were later connected by the headward erosion of the Yellow River (Pan et al., 2011).

The considerable accumulation of aeolian sediments within the region serves as an exceptional repository of climatic information (Ao et al., 2017; Peng et al., 2018). A previous study investigated the fluctuations in goethite concentration within aeolian sediments at the Chaona profile on the Chinese Loess Plateau, revealing a distinct pattern of intensified East Asian Summer Monsoons, featuring augmented precipitation, during the Late Miocene to Early Pleistocene (Zhang et al., 2017). This intensified monsoonal activity probably contributed to increased surface runoff and expedited landscape evolution processes.

3. Geomorphic sequences and sedimentary characteristics along the northern Jinshaan Gorge

The top of the Baode paleolake sedimentary sequence is unconformably overlain by Red Clay and subsequent loess, at altitude comparable with those at which the aeolian sequences overlies weathered limestone bedrock. The uppermost fluvio-lacustrine Baode deposits, together with the weathering crusts capping the limestone, form the main body of the Tangxian-period planation surface (Pan et al., 2011). Investigation of the Baode paleolake has centered on the analysis of cross sections between Gaojiayinze and Luzigou (G–L) and between Gaojiayinze and Dayandun (G–D), with extensive fieldwork. By establishing connections between the boundary of the fluvio-lacustrine deposit with the bedrock, a rough estimation of the spatial extent of the Baode paleolake was obtained.

Our fieldwork along the Yellow River channel from south to north up to the Hetao Basin revealed that remnants of river gravels and overlying Red Clay are commonly distributed above the northern Jinshaan gorge. They are situated on or slightly below the level of the Tangxian-period planation surface, at an elevation is close to the top of the fluvio-lacustrine deposition in the Baode area. We found that the gravels can be divided into two distinct units at different elevations, G1 (the lower one) and G2 (Fig. 2).

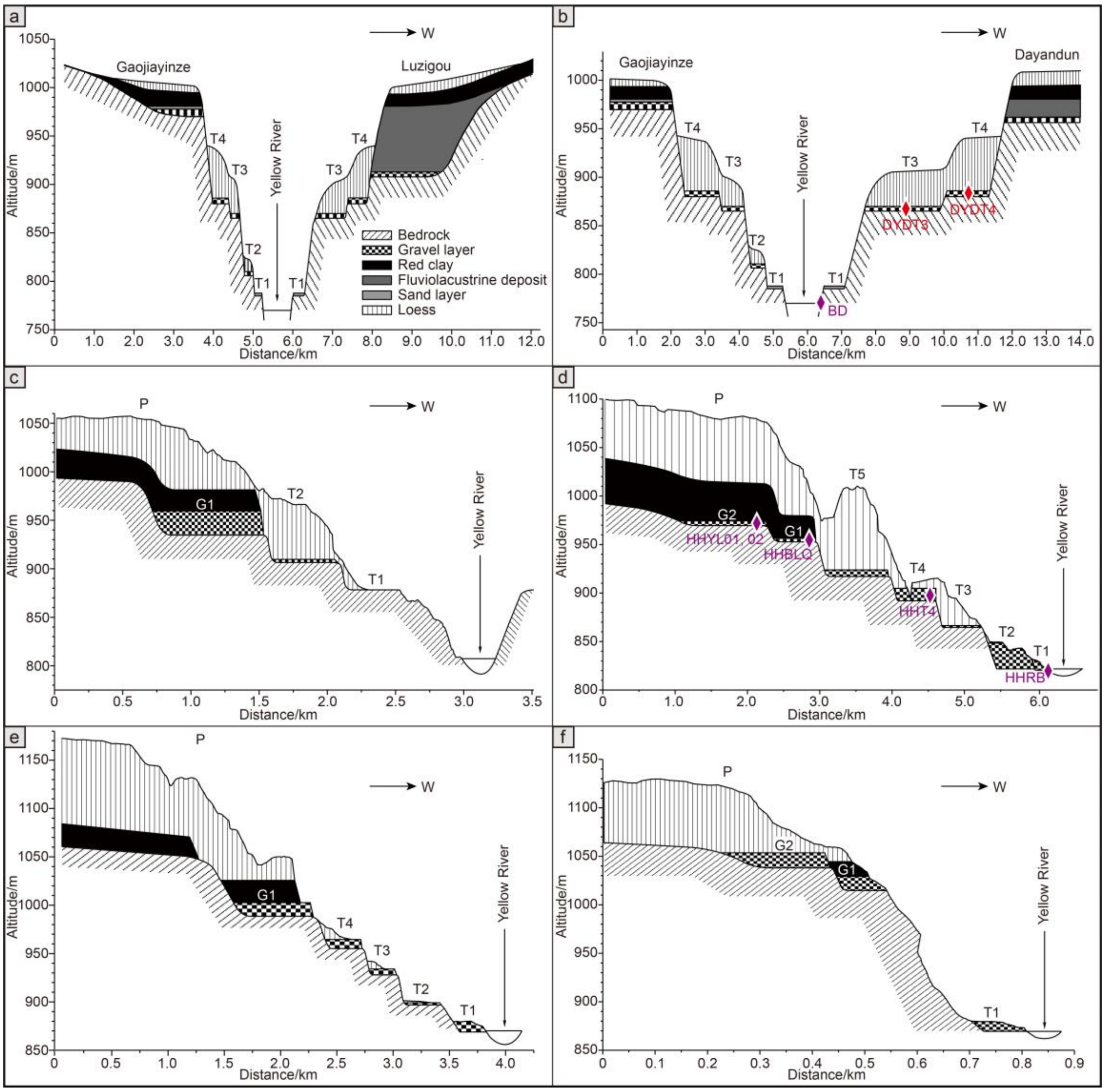

Figure 2. Schematic cross-section of fluvial terraces along the Jinshaan Gorge (see **Fig.1b** for location). a.) Gaojiayinze–Luzigou (G–L) section, b.) Gaojiayinze–Dayandun (G–D) section, c.) Huangyuya section, d.) Hequ section, e.) Guanhekou section, f.) Wanjiazhai section. Sample sites and published sites marked by red and purple diamonds respectively.

The uppermost surface of the higher gravel unit (G2) is 184–150 m above the level of the Yellow River. This gravel layer is 5 m thick and is overlain by 4 m of overbank silt and then up to 28 m of Red Clay. This sequence is capped by aeolian loess, characteristic of the region. The gravel clasts range between 2 and 10 cm diameter, with limestone being the dominant lithology, and shows clear imbrication. Magnetostratigraphic dating of the lowermost Red Clay accumulation above the gravel establishes that its formation predates ~4.9 Ma (Pan et al., 2011), indicating a minimum age for the gravel.

The top of the lower (G1) gravel is 160–133 m above the level of the Yellow River. This gravel is 2 m in thick and is overlain by about 15 m of Red Clay, with a further cover of aeolian loess. The gravel clasts are generally 2–7 cm, again are mainly limestone, with an imbricated arrangement. The basal of Red Clay above the G1 gravel is dated to 3.7 Ma (Pan et al., 2011).

Three longitudinal sections, named after Huangyuya, Guanhekou, and Wanjiazhai, were carefully traced along these two gravel units from the Baode paleolake in the south to the Hetao Basin in the north (Fig. 1b, Fig. 2). We conducted measurements of the gravel units' surface elevation for each section, relative to the river. These measurements were then compared with the G–L, G–D, and Hequ sections, which were previously published, allowing a comprehensive assessment of the morphological consistency within the studied region. Two terraces are preserved below the G1 gravel in the Huangyuya section, both of which are strath terraces with Quaternary loess directly overlying their gravels. The Guanhekou section preserves a total of four Yellow River terraces. While the lowest (T1) is a fill terrace, the remainder are strath terraces, with subsequent deposition of Quaternary loess. In the Wanjiazhai section, only a single fill terrace is preserved.

Preservation of the G1 and G2 gravel and the more recent Yellow River terraces does not occur uniformly across all sections. However, a Swath plot reveals that, despite the variations, these features exhibit significant comparability, leaving no doubt that they collectively represent geomorphic records of rivers oriented in a north-south direction. In order to validate whether they belong to a singular river system, we undertook further investigations.

4. Material and methods

4.1 Investigation and sampling sites

To reconstruct the evolution of the drainage system, first, the establishment of a comprehensive chronological framework is essential and, second, an analysis of sediment composition is crucial for revealing the source–sink pattern. The study area benefits from previous paleomagnetic dating (Pan et al., 2011), which has successfully established a robust chronological framework for the aeolian sediments deposited above the gravels. Nonetheless, there remains a lack of quantitative investigations concerning the lithological composition and provenance of these gravels.

We investigated the following sections (from south to north, respectively) in detail: G–L (39°01′21″ N,111°09′38″E), G–D (38°58′41″N,111°05′21″E), Huangyuya (39°07′26″N,111°10′44″E), Hequ (39°23′20″N,111°08′13″E), Guanhekou (39°29′32″N,111°24′39″E), and Wanjiazhai (39°34′08″ N,111°25′59″E). The elevation and thickness of the gravel bodies and of overlying overbank and aeolian sediments were measured using high-precision differential GPS (Trimble GEO 7X). The Hequ section has been studied previously for gravel lithology and zircon U–Pb chronology (Xiong et al., 2022), and our present study extends these investigations to encompass each section located at the northern extremity of the Jinshaan Gorge, employing both analysis of gravel lithology and paleocurrent measurement. Furthermore, recent provenance studies of the middle and lower reaches of the Yellow River using zircon U–Pb chronology have provided much evidence for the reconstruction of drainage evolution (Kong et al., 2014; Nie et al., 2015; Xiao et al., 2020; Zhang et al., 2021). In our present study, we conducted a provenance study for the fluvio-lacustrine deposits in the Luzigou section and the Yellow River terrace sediments in the G–D section.

As previously described, the Luzigou section (39°01′21″N,111°09′38″E) is the sedimentary center of the Baode paleolake, where fluvio-lacustrine deposits have accumulated since the Late Miocene (Pan et al., 2011), attaining a thickness of up to 77 m, stacked unconformably above the underlying Carboniferous sandstone (Fig. 3). At their base is a distinct set of fluvial gravel unit, measuring approximately 10 m in thickness. These gravels are highly abraded, predominantly showing a sub-rounded morphology, with clast diameters 2–10 cm. Their lithological composition is exceptionally homogeneous, with nearly 98% limestone. They are distinctly imbricated and incorporate mud lenses, signifying that they represent fluvial deposition with stable channels. Sample LZGD was taken at the bottom of this gravel layer. The overlying fluvio-lacustrine strata primarily comprise mudstone, siltstone, and sandstone, with a cumulative thickness of ~67 m. Notably, another distinct gravel unit, which is inset into the fluvio-lacustrine sequence and with the same lithology as G2 found on the planation surface, occurs 30 m below the top surface with a thickness of 3 m. Along the profile, from the bottom upwards, we collected detrital samples LZG11, LZG9, LZG8 and LZG6 (Fig. 3). Based on previous chronological investigations, the ages of LZGD, LZG11, LZG9, LZG8, and LZG6 correspond to paleomagnetic ages of approximately 10 Ma, 7.1 Ma, 5.2 Ma, 4.9 Ma, and 3.7 Ma, respectively (Pan et al., 2011).

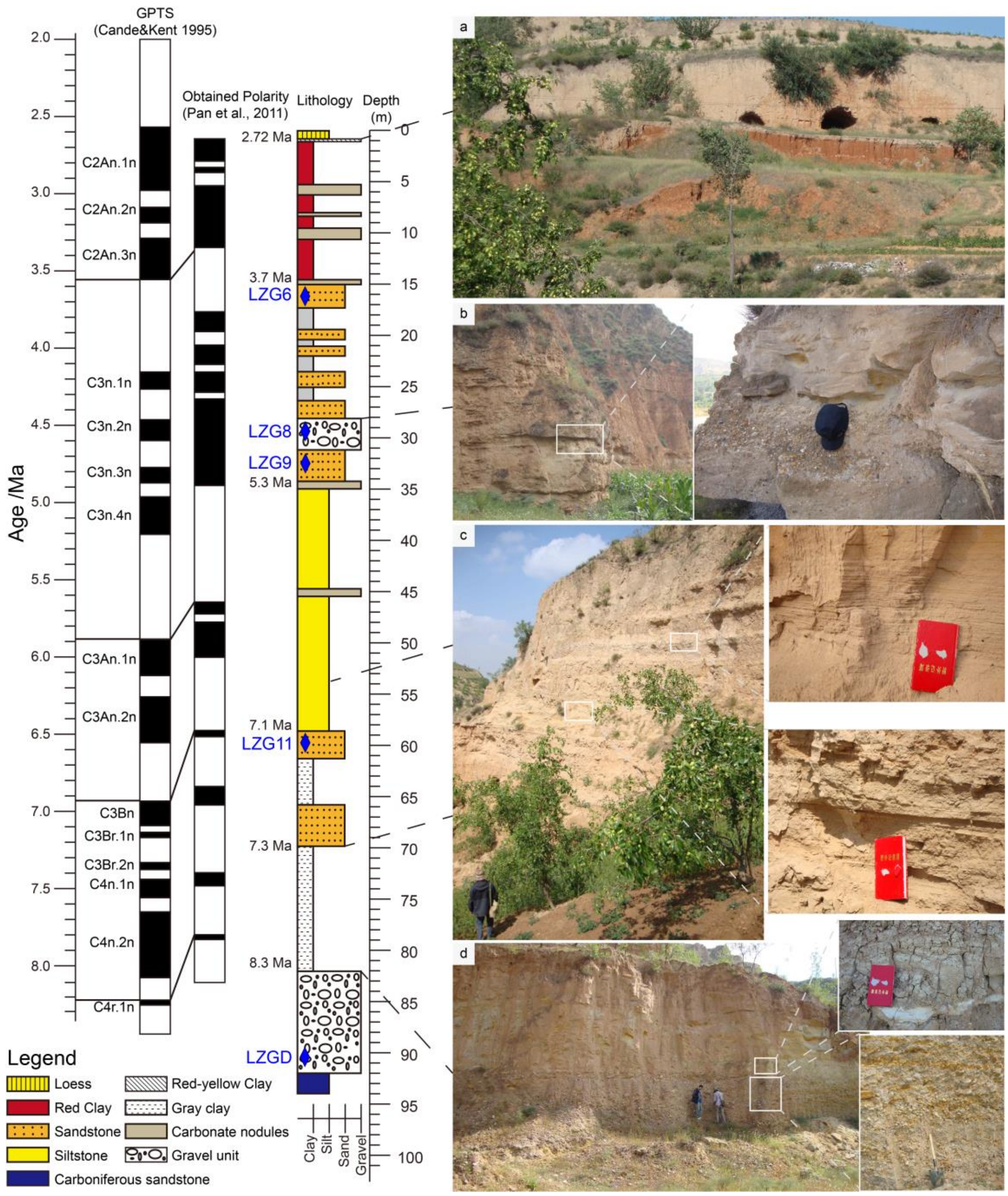

Figure 3. Magnetostratigraphy, pedostratigraphy and field photos of the Luzigou section in the Baode area. Zircon U–Pb samples location marked by pale green diamonds. a.) The loess–Red Clay boundary. b.) The higher gravel unit. c.) Two sand layers in the middle section. d.) Lacustrine strata and lowest gravel unit in the basal section. For chronological framework, lithological description, and interpreted chrons (black and white for normal and reverse geomagnetic polarities) for see Pan et al. (2011).

4.2 Sedimentary analyses

We measured the lithological composition of the G1 and G2 gravels across all sections, as well as for the gravel unit within the Baode fluvio-lacustrine sequence. Additionally, paleocurrent were measured in the G1 and G2 gravels in the Huangyuya, Hequ, Guanhekou, and Wanjiazhai sections, as well as within the Yellow River terrace gravels in the Hequ section. The lithology and preferred orientation (imbrication) of >100 gravel clasts were measured for each sample, which was observed on the gravel unit outcrops. The size range of measured clasts is >3 cm in b-aixs. The gravel-forming geology and resultant clast lithologies in the study area are relatively homogeneous, primarily comprising limestone, sandstone, quartzite, quartzitic sandstone, mudstone, slate, and phyllite. To obtain imbrication, we measured the inclinations of the a-b surfaces of the gravel clasts, which corresponds to the upstream direction, and plotted the rose diagrams and preferred orientation using the software PC99 (Woolfe et al., 2000). Figure 4 shows three-dimensional pie charts depicting the distribution of gravel lithology, as well as paleocurrent rose diagrams (in which flow direction is denoted by the red arrow).

4.3 Detrital zircon pretreatment

Samples were wet sieved to isolate the 15–250 μm fraction, from which zircon grains were separated using standard dense-liquid techniques. Zircon grains were randomly selected under a binocular microscope and mounted using epoxy resin. Pretreatment was carried out at the Key Laboratory of Mineral Resources in Western China (Gansu Province), School of Earth Sciences, at Lanzhou University, China.

4.4 U–Pb geochronological measurement

Detrital-zircon dating was carried out by means of inductively coupled plasma mass spectrometry (ICP-MS) using an Agilent 7700x instrument with an attached CETAC Analyte Excite Excimer Laser Ablation System, at the Department of Geography, Nanjing Normal University, China. The laser beam diameter was set to 20 μm and, as standard reference materials, zircon 91500 (Wiedenbeck et al., 1995), GJ- 1(Jackson et al., 2004), Plešovice (Sláma et al., 2008), and QH (Li et al., 2009) were used. For zircons younger than 1000 Ma, we used $^{206}Pb/^{238}U$ ages, whereas $^{206}Pb/^{207}Pb$ ages were used for zircons older than 1000 Ma, with uncertainties expressed at 2σ. Samples with >10% discordance were not considered (see full data provided as Supplementary Material).

Data are presented as kernel density estimation plots (KDEs) and non-matrix multi-dimensional scaling (MDS) maps, using the software IsoplotR (Vermeesch, 2012, 2013), were used for provenance interpretation.

5. Results

5.1. Lithological composition and paleocurrents

Data on gravel clast lithology, paleocurrent and elevation profiles of geomorphic surfaces were combined and plotted on the Swath diagram of the northern Jinshaan Gorge (Fig. 4). The lithological composition of gravels within the Baode paleolake sequence and the high-level G1 and G2 gravels is predominantly limestone, exhibiting a more homogeneous distribution in the southern section of the study area. This lithological pattern changes to sandstone, quartzitic sandstone, and quartzite components in the northern section. In contrast, the lithological composition of Yellow River gravels in the Hequ section shows a gradual but progressive change in composition from the higher to lower terraces with sandstone, quartzite and limestone, significantly differing from the lithology observed in G1, G2 and Baode paleolake gravels with predominant limestone.

This notable dissimilarity is further highlighted in the paleocurrent patterns. The inclinations of the a-b surfaces of the gravel clasts within the Yellow River terraces predominantly exhibit a single direction towards the north, suggesting consistent paleoflow from north to south, conforming with the present-day course of the Yellow River. In contrast, the inclinations of the a-b surfaces of the G1 and G2 gravel clasts display a relatively mixed distribution, with a predominant southward trend. This indicates a reversal of drainage in comparison with the modern Yellow River.

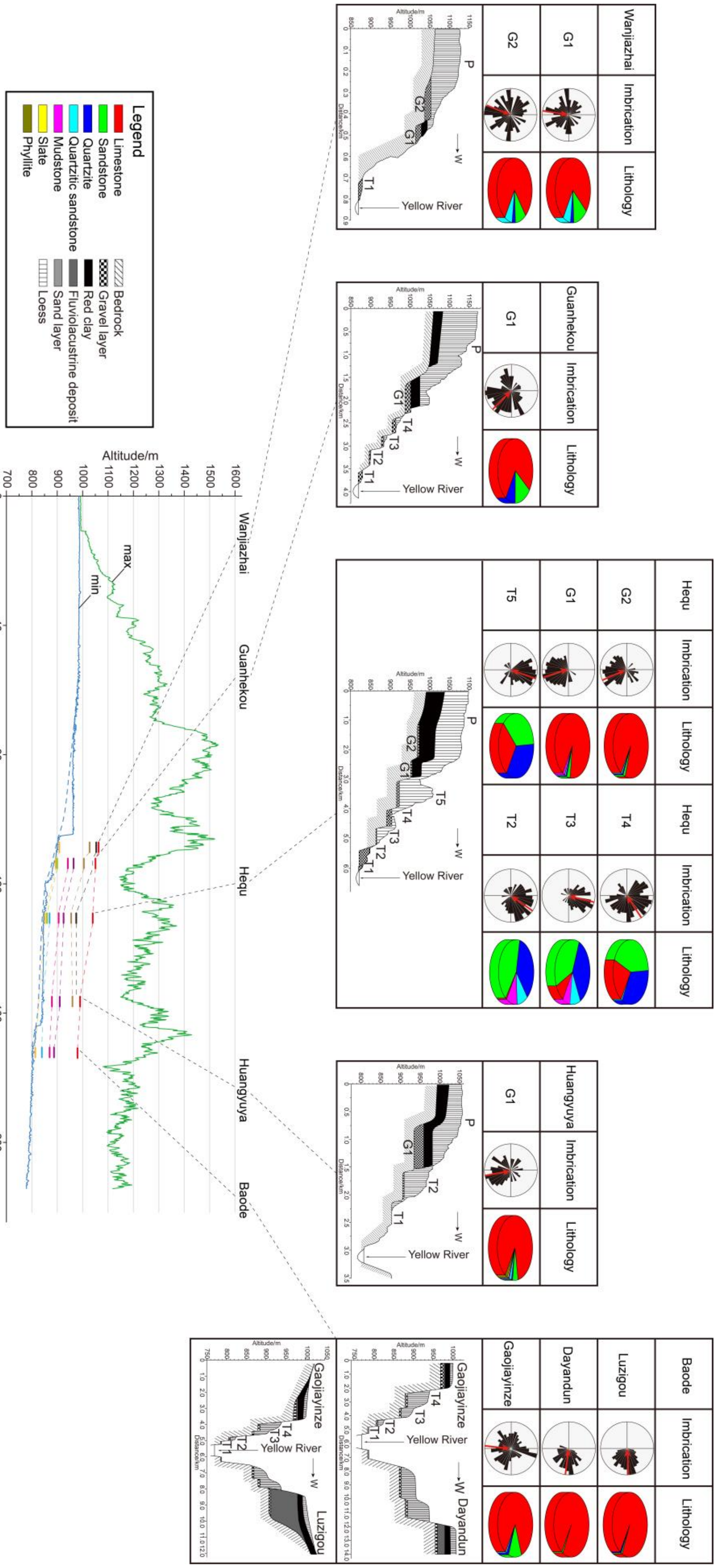
Legend
Limestone
Sandstone
Quartzite
Quartzitic sandstone
Mudstone
Slate
Phyllite
Bedrock
Gravel layer
Red clay
Fluviolacustrine deposit
Sand layer
Loess
Altitude/m
Distance/km
max
min
Wanjiazhai
Guanhekou
Hequ
Huangyuya
Baode
Imbrication
Lithology
G1
G2
T1
T2
T3
T4
T5
P
W
Yellow River
Luzigou
Dayandun
Gaojiayinze

Figure 4. The 3D pie charts showing gravel clast lithology, rose diagrams showing paleocurrent directions, and elevation profiles of geomorphic surfaces, all plotted onto the Swath diagram of the northern Jinshaan Gorge of the Yellow River. Maximum and minimum elevation along a 25-km-wide swath window (perpendicular to swath transect), the location of which is shown in Fig 1a.

5.2. Zircon U–Pb chronological spectrum

KDE plots are utilized to illustrate the zircon U–Pb spectrum (Fig. 5). In order to facilitate the analysis, our samples are plotted alongside those of previous authors, allowing comprehensive comparison and examination of the data. Sample LZGD shows dominant peaks at ~2500 Ma, and minor peaks at ~250 Ma and ~2500 Ma. Sample LZG11 has subequal dominant peaks at ~250 Ma and ~450 Ma, with minor peaks at ~800 Ma, ~1800 Ma and ~2500 Ma. Sample LZG9 displays dominant peaks at ~250 Ma and ~1800 Ma, a lower peak at ~450 Ma, and minor peaks at ~800 Ma and ~2500 Ma. Sample LZG8 and LZG6 show dominant peaks at ~1800 Ma, and lower peaks at ~250 Ma and ~2500 Ma. The Yellow River terraces (samples from DYDT4 and DYDT3) display subequal peaks at ~1800 Ma, ~250 Ma, and ~2500 Ma, like the spectrum of Yellow River terrace T4 in Hequ (HHT4).

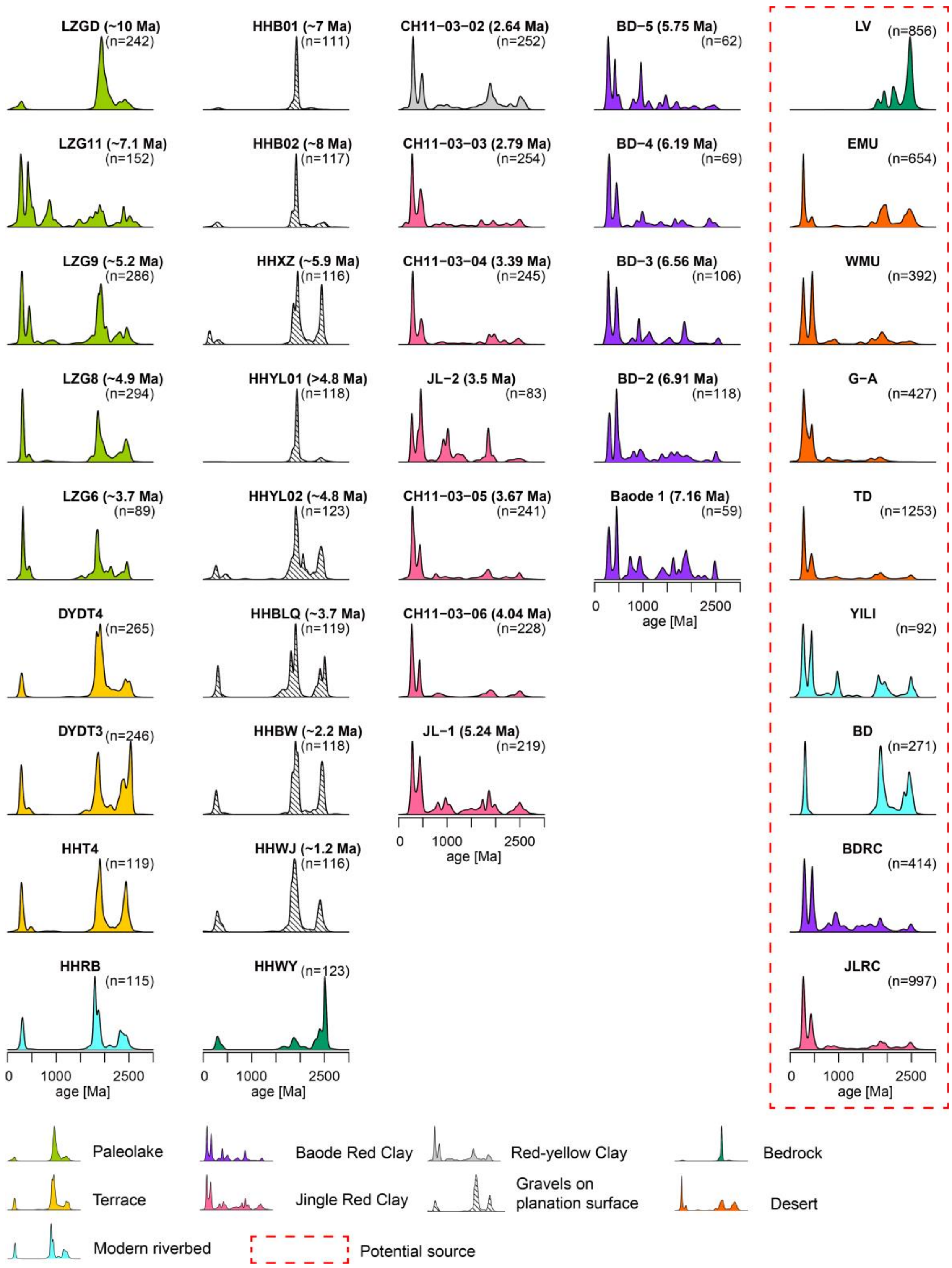

Figure 5. KDE plots of U–Pb zircon-age data, published data from Zhao et al. (2008), Stevens et al. (2010, 2013), Liu et al. (2011), Liu et al. (2012), Wang et al. (2014), Nie et al. (2015), Licht et al. (2016), Shang et al. (2016), Zhang et al. (2016, 2021), Xiong et al. (2022), Bohm et al. (2023) (full datasets provided as Supplementary Material).

6. Discussion

6.1 Drainage reconstruction on the planation surface

Gravel fabric analysis has been widely employed in fluvial evolution studies within sedimentary records of river terraces (Rust, 1972; Miao et al., 2008; Souza et al., 2022). The rose diagrams provide valuable insights into local paleocurrents, indicating that a river different from the modern Yellow River flowed from south to north across the study area during the peneplanation period. The chronological analysis of the G2 gravel unit suggests that this river system existed during the early Pliocene (minimum age 4.9 Ma). The sediment chronology of the Hetao Basin reveals deposition in the eastern part of the basin since at least the Late Miocene, with a hiatus indicated by an unconformity dated ~5.3 Ma (Shi et al., 2020). On the basis of the aforementioned evidence, we propose that the process of drainage integration events began at this time, with the fluvial outflow from the Baode paleolake, prior to which this was probably a long-term endorheic lacustrine system. The Yellow River traversed the Hetao Basin prior to entering the Jinshaan Gorge, depositing gravels and coarse sands from the upper reaches (Nie et al., 2015), and the gravels within the gorge predominantly originate from the adjacent mountainous regions. Specifically, these gravels comprise limestone sourced from the Ordovician strata of the Lüliang Mountains, while the sandstone predominantly originated from the Triassic and Cretaceous strata of the Ordos block.

Zircon KDE plots can provide valuable insights into drainage evolution, revealing similar patterns indicated by the gravel-forming geology and resultant clast lithologies (Fig. 5). The LZGD samples exhibit striking similarities to samples HHB01, HHB02, and HHYL01 of Xiong et al. (2022), which suggests a common provenance from the Lüliang Mountain. This observation aligns with the low-temperature thermal age evidence in indicating rapid uplift of the Lüliang Mountains at ~12 Ma

(Zhao et al., 2016). It is highly likely that the uplift of the Lüliang Mountains, coupled with the extensive lateral river system in the western piedmont, facilitated the deposition of these gravels in lower parts of the peneplain. This deposition is also evident in the Liulin area within the middle Jinshaan Gorge (Li et al., 2009).

A distinct variation in provenance is evident between LZGD and LZG11, with the latter displaying a more diverse spectrum characterized by peaks at ~250, ~450, ~800, and ~2500 Ma. No zircon spectra like LZG11 were found in sediment samples from the geomorphic surfaces in the Hequ section. However, it is noteworthy that the sample LZG11 exhibits remarkable similarities to the Late Miocene Red Clay deposits in the Baode area (Shang et al., 2016; Bohm et al., 2023). This multi-peak pattern probably signifies the presence of materials originating from the Central Asian Orogen Belt and transported over long distances by East Asian Winter Monsoon. The chronologies of multiple sedimentary sequences suggest that aeolian deposition to the east of the Liupan Mountains may have commenced around 7 Ma (Sun et al., 2022). The sample LZG11 represents a period characterized by increased aridification in inland Asia, leading to enhanced aeolian deposition and supply of material to the Baode region, as well as deposition in the Baode Paleolake through slope erosion and transportation by flowing water.

Comparing LZG9 to LZG11, it is evident that LZG9 exhibits higher peaks at ~200 Ma and ~1800 Ma. This coincides with the Miocene–Pliocene transition and the shift from Baode Red Clay to Jingle Red Clay deposition in the Baode area (Zhu et al., 2008). The significantly wetter climatic conditions during this period led to increased surface runoff (Ao et al., 2021), enhanced local erosion capacity, and a greater contribution of materials from the East Mu Us (EMU) desert and the Lüliang Mountains. Samples LZG8 and LZG6 both reflect a similar provenance, characterized by a mixture of materials originating from the Lüliang Mountains and EMU, in alignment with the sediment composition found on the planation surface of the Hequ section.

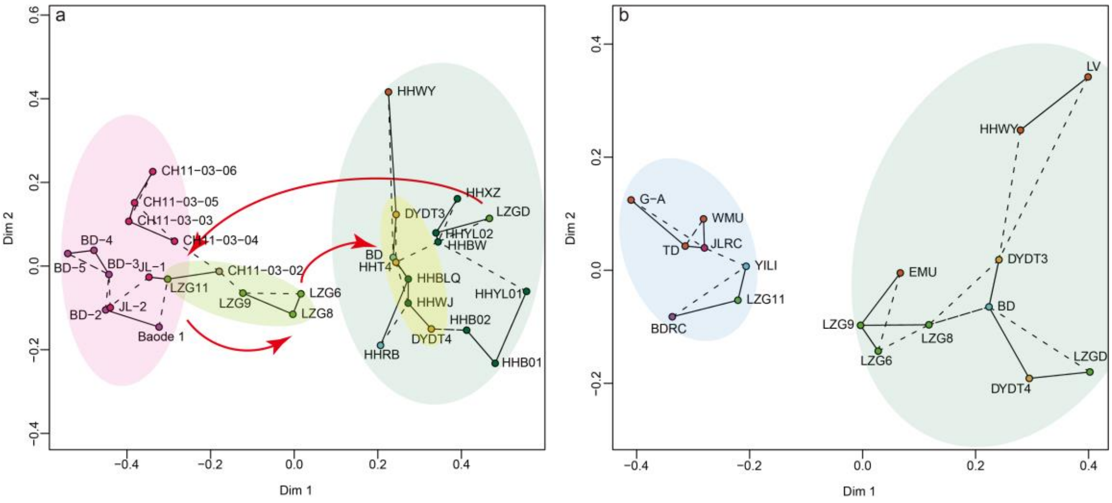

Figure 6. Non-matrix multi-dimensional scaling (MDS) plot of U–Pb zircon-age data. The proximity between samples reflects their degree of similarity, with solid lines connecting them denoting the first level of similarity, while dashed lines represent the second level of similarity. Colored areas represent main potential sources (Red=Red Clay, Green=Lüliang mountains and Ordos Block, Pale Green=Luzigou section, Yellow=Yellow River terraces, Blue=Central Asian Orogenic Belt and Tibetan Plateau) a.) Sediment similarity relationship between the Baode and Hequ regions. b.) The similarity of samples to potential source regions.

Incorporating MDS plots, our findings reveal two significant changes in provenance within the Luzigou section during the peneplanation period (Fig. 6). The first change occurred after the initial accumulation of fluvial gravel, whereas the second occurred before the formation of the G2 gravel unit at ~4.9 Ma. The basal gravel unit of the Luzigou fluvio-lacustrine strata signifies an inland water system characterized by a relatively simple provenance. However, due to the fine grain size of the lacustrine clay above the basal gravel unit, conducting zircon U–Pb chronology becomes challenging. Consequently, it proves difficult to determine the duration of the single provenance process and how the source evolved before 7.1 Ma, after which a change in provenance occurred prior to 4.9 Ma, which we attribute to intensified erosion resulting from increased climatic humidity (Ao et al., 2021). Enhanced runoff due to climatic humidity may have brought in more detrital, replacing a pattern dominated by aeolian deposition. Concurrently, we can discount additional provenance changes in the local area resulting from potential alterations in the source of the Red Clay. Within the Baode region, variation in the source of Baode Red Clay and Jingle Red Clay during this period is comparatively minor compared to fluctuations observed in the fluvio-lacustrine sediments (Shang et al., 2016; Bohm et al., 2023) and is thus inadequate as an explanation of provenance variation within the Luzigou section. In contrast, the analysis of Red Clay provenance in the Jiaxian section may offer greater insights into the formation of the north-flowing fluvio-lacustrine system of the Baode paleolake and its role in supplying weathered materials to the downwind Red Clay deposits (W.B. Peng et al., 2023).

Furthermore, previous studies suggest continuous and sequential accumulation of aeolian sediments in the Baode area, extending back to at least 7.1 Ma (Zhu et al., 2008), sediments that probably represented a consistent supply of material to the Baode Paleolake. The observed changes in sediment provenance can be attributed to increased contributions of silt- to sand-size detritus from local rivers. It is important to note that the zircon U–Pb method exhibits greater sensitivity to this grain size, owing to inherent limitations of the technique itself. Consequently, the influx of fluvial material gradually replaced the previously eroded local Red Clay, assuming a dominant role within the sedimentary record of the Baode Paleolake.

6.2 Provenance of sediments of the integrated Yellow River

The sediment provenance of the modern Yellow River bedload gravel has been a subject of significant interest and investigation among geologists due to the discovery that provenance may exhibit spatial variability across different sections of the river (Kong et al., 2014; Nie et al., 2015). In these studies, there has been focus on the Hetao Basin to Baode region, located around the northern part of the Jinshaan Gorge, where notable provenance variations have been observed, as exemplified by samples YILI and BD of Nie et al. (2015). Furthermore, the sediment provenance in the Yumenkou area at the southern end of the Jinshaan Gorge shares similarities with the BD samples, indicating a local source from the Ordos Block and the adjacent Lüliang Mountains (Kong et al., 2014). These findings suggest that the contemporary processes governing sediment transport in the middle reaches of the Yellow River system impede the passage of materials originating from the Tibetan Plateau through the Jinshaan Gorge. Consequently, these materials fail to reach downstream regions such as the North China Plain or the Bohai Sea. This observation highlights the complex dynamics of sediment transport and underscores the need for a comprehensive understanding of sediment provenance across different sections of the Yellow River system.

The investigation of zircon-age spectrums in the terrace gravels of the Hequ section has yielded crucial insights into the temporal extent of the sediment transport process, suggesting a possible duration from the terrace HHT4 formed (0.1 Ma) to present (Xiong et al., 2022). Notably, the analysis of samples DYDT4 and DYDT3 in this study, in combination with data from previously published samples YILI, BD, HHRB, and HHT4, reveals that material sourced from the upper reaches of the Hetao Basin has been impeded in reaching the Baode area since the initial formation of the integrated Yellow River. This timeframe pre-dates the formation of the highest Yellow River terrace, estimated at 1.2 Ma, based on previous paleomagnetic chronostratigraphy (Pan et al., 2012).

These findings suggest that the disruption in sediment transport from the upstream Hetao Basin to the Baode area occurred prior to the formation of the highest terrace, indicating prolonged restriction in sediment transport during this earlier period.

6.3 Drainage reorganization along the Jinshaan Gorge recorded by the provenance change

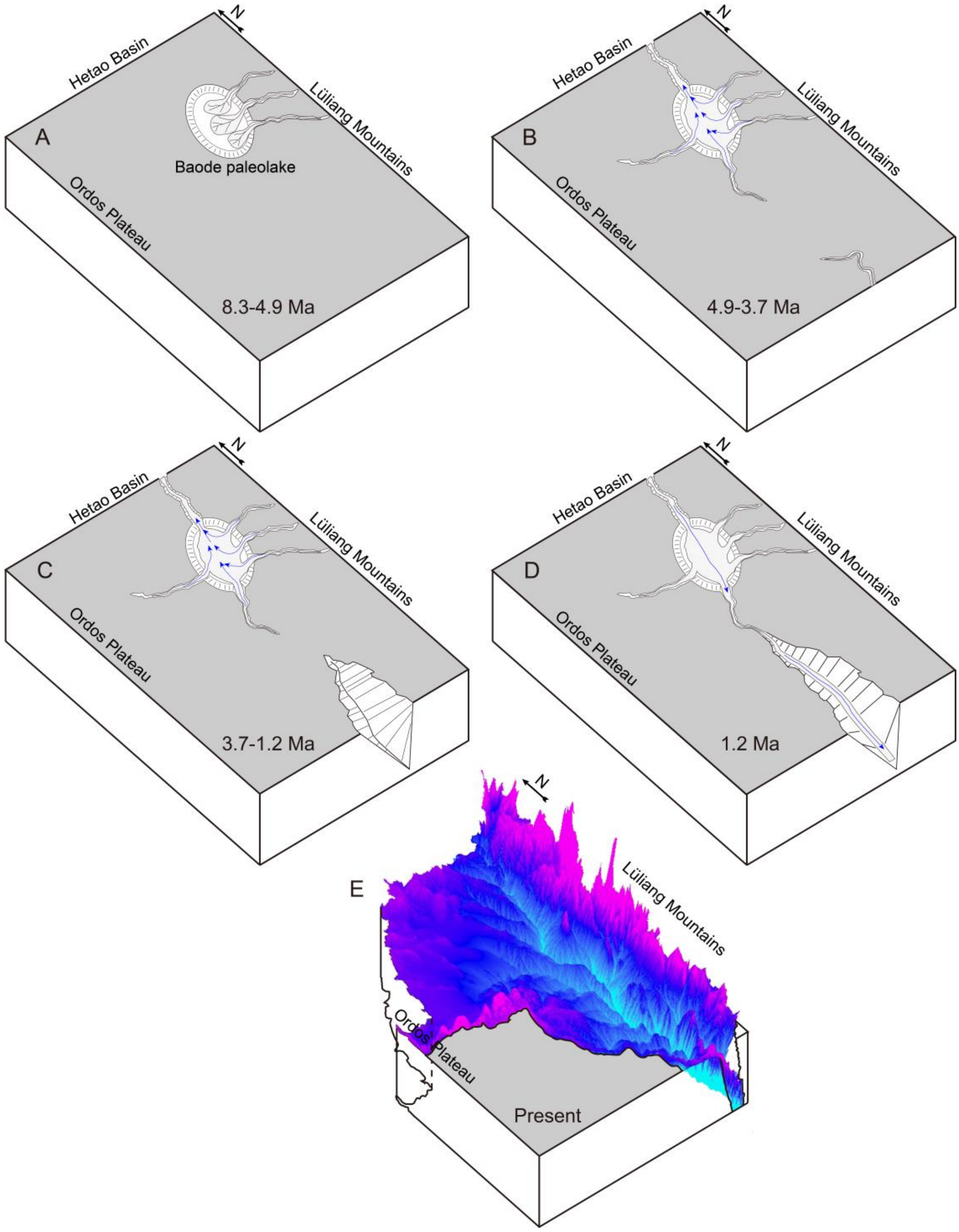

Figure 7. Time-slice sketch of evolutionary model in the northern Jinshaan Gorge since the Late-Miocene.

Our study has revealed noteworthy distinctions in provenance between the fluvio-lacustrine (LZG8 and LZG6) and terrace samples (DYDT4, DYDT3, and HHT4). Although the visual disparity on the KDE plots may not be obvious, a significant increase in the ~1800 Ma peak introduces a distinct separation between these two datasets on the MDS plots (Fig. 6). This disparity in provenance can be attributed to the intensified hydrodynamics following the formation of the integrated Yellow River, in which the reworking of Red Clay into fluvial deposits became limited. In contrast, the terrace samples exhibit a simpler local source that aligns with the characteristics of modern riverbed samples.

In this study, we present a comprehensive model for drainage evolution in the northern section of the Jinshaan Gorge, as illustrated in Figure 7. During the peneplanation period, from 8.3 to 4.9 Ma, a depression existed in the Baode area, resulting in the deposition of fluvio-lacustrine strata in the Baode paleolake, the main sediment source being the Red Clay. At 4.9 Ma, continued increasing of climatic humidity led either to the overflow of the lake or an inland river flowing into the Hetao Basin eroded headward and incised through the paleolake, giving rise to a paleo-river that flowed in the opposite direction to the modern Yellow River. Subsequently, at 3.7 Ma, the dissection of the Tangxian-period planation surface triggered increased fluvial erosion, so that rivers originating from the Fenwei Basin began to erode northward along the western piedmont of the Lüliang Mountains as the headward erosion pattern in Hu et al. (2016). This pattern of headward erosion is similar to that proposed by the previous study in Sanmen Gorge (Liang et al., 2022). And the erosion process persisted until 1.2 Ma, when there was finally fluvial incision through the Baode area, resulting in the formation of the modern Yellow River. Concurrently, the initiation of the Jinshaan Gorge occurred, followed by the progressive incision that led to the formation of the Yellow River terrace sequence.

In conclusion, we emphasize that the formation of the modern configuration of the Yellow River in the Jinshaan Gorge occurred between 3.7 Ma and 1.2 Ma, following the dissection of the planation surface and preceding the formation of the highest terrace. Varied interpretations of the remaining sediments within the gorge have resulted in divergent views on the timing of Yellow River formation in previous studies. One of the viewpoints suggests that the fluvio-lacustrine sediments overlying the planation surface can probably be interpreted as the archive of ancient Yellow River, excavating a wide valley by lateral erosion through the whole Jinshaan Gorge in the period from 8 to 3.7 Ma (Liu, 2020; Li et al., 2022; Xiong et al., 2022). In contrast, more evidences from terrace correlation and lithological composition argue an independent origination between the fluvio-lacustrine sediments accumulated on planation surface and the Yellow River terraces (Cheng et al., 2002; Pan et al., 2012; Hu et al., 2016, 2017, 2019). The comprehensive provenance study here seems to be correspondent to the latter, concluding that the fluvio-lacustrine deposits on the Tangxian-period planation surface probably represent distinct endorheic drainage system during peneplain development across the northern Jinshaan Gorge, rather than being attributable to the modern integrated Yellow River. First, their distribution lacks connectivity and is difficult to relate to other parts of the Jinshaan Gorge area parallel to the Yellow River. Second, comprehensive provenance evidence in support of their association with more modern Yellow River deposits is lacking. While our study focuses primarily on the provenance differences between sediments overlying the planation surface and those of the modern Yellow River in the northern part of the Jinshaan Gorge, further investigations encompassing the entire gorge are clearly warranted. Nonetheless, it is evident that the presence of the Yellow River in the northern segment of the Jinshaan Gorge postdates 3.7 Ma.

We also would like to highlight an interesting observation regarding the headward erosion of the Yellow River during the period from 3.7 to 1.2 Ma. Our analysis reveals a distance of headward erosion during this period of ~410 km, at an average rate of 164 km/Ma (Hu et al., 2016). It is important to note that this erosion rate is significantly less than the headward-erosion rate of 350 km/Ma calculated by Craddock et al. (2010) for the Yellow River in the northeastern Tibetan Plateau. This discrepancy may be attributed to the different tectonic backgrounds of the two regions, with more active tectonic uplift in the northeastern Tibetan Plateau. Furthermore, numerous drainage reorganization archives originated from the global view all appear to occur in the Plio-Pleistocene period (Gouveia et al., 2020; Yang et al., 2021), yielding a remarkable correlation with the worldwide warming and wetting climate (Nie et al., 2014; Freitas et al., 2022). The process of drainage reorganization can vary based on the specific tectonic, climatic, and geomorphological settings, emphasizing the need to consider these factors holistically when reconstructing evolutionary history. Incorporating these elements into the analysis will contribute to a more comprehensive understanding of the complex reorganization processes associated with drainage in different regions.

7. Conclusions

Taking into consideration the spatial distribution of geomorphic surfaces, sedimentary characteristics, and provenance analysis, we have reconstructed the evolutionary history of the northern section of the Jinshaan Gorge from the peneplanation period to the development of the modern deeply incised valley of the Yellow River. Our investigation encompasses Late Miocene to Early Pleistocene time, capturing key provenance changes within this timeframe. The Baode paleolake emerged around 8.3 Ma as a localized endorheic system. Subsequently, at ~4.9 Ma, it became established as a fluvio-lacustrine system in conjunction with the Hetao Basin, resulting in northward outflow. As this process continued, the enhanced erosion resulting from the formation of the planation surface at ~3.7 Ma further reshaped the landscape. Finally, at 1.2 Ma, the downstream river captured the fluvio-lacustrine system, forming the present-day Yellow River middle reaches. Our study provides a robust framework that offers a comprehensive and reliable explanation for the evolution of the middle Yellow River catchment, taking into account the significant influences of increasing climatic humidity and relative tectonic uplift.

Acknowledgments

This article is dedicated to the memory of Prof. Rob W.C. Westaway, a distinguished geologist and geomorphologist. We thank Prof. Martin Gibling for reviewing and improving the initial version of this manuscript. This research was financially supported by the National Natural Science Foundation of China (Grant no. 42041006; Grant no. 42371001), the Fundamental Research Funds for the Central Universities, China (lzujbky-2022-ey10), and 111 Program from State Administration of Foreign Experts Affairs and Ministry of Education of the People's Republic of China (Grant no. BP2018001).

References

Ao, H., Rohling, E.J., Zhang, R., Roberts, A.P., Holbourn, A.E., Ladant, J.B., Dupont-Nivet, G., Kuhnt, W., Zhang, P., Wu, F., Dekkers, M.J., Liu, Q.S., Liu, Z.H., Xu, Y., Poulsen, C.J., Licht, A., Sun, Q., Chiang, O., Liu, X.D., Wu, G.X., Ma, C., Zhou, W.J., Jin, Z.D., Li, X.X., Li, X.Z., Peng, X.Z., Qiang, X.K., An, Z.S., 2021. Global warming-induced Asian hydrological climate transition across the Miocene-Pliocene boundary. Nat. Commun., 12(1). https://doi.org/10.1038/s41467-021-27054-5.

Bar, O., Zilberman, E., Feinstein, S., Calvo, R., Gvirtzman, Z., 2016. The uplift history of the Arabian Plateau as inferred from geomorphologic analysis of its northwestern edge. Tectonophysics, 671, 9-23. https://doi.org/10.1016/j.tecto.2016.01.004.

Bohm, K., Kaakinen, A., Stevens, T., Lahaye, Y., Tang, H., Shang, Y., Zhang, H.Z., Lu, H.Y., 2023. Neogene global climate change and East Asian dust sources: Combined rutile geochemistry and zircon U-Pb analysis from the northern Chinese Loess Plateau. Global Planet Change, 221, 104049. https://doi.org/10.1016/j.gloplacha.2023.104049.

Cheng, S.P., Deng, Q.D., Zhou, S.W., Yang, G.Z., 2002. Strath terraces of Jinshaan Canyon, Yellow River, and Quaternary tectonic movements of the Ordos Plateau, North China. Terra Nova, 14(4), 215-224. https://doi.org/10.1046/j.1365-3121.2002.00350.x.

Craddock, W.H., Kirby, E., Harkins, N.W., Zhang, H.P., Shi, X.H., Liu, J.H., 2010. Rapid fluvial incision along the Yellow River during headward basin integration. Nat. Geosci., 3(3), 209-213. https://doi.org/10.1038/ngeo777.

Davis, W.M., 1899. The geographical cycle. Geographical J., 14(5),481–504. http://www.jstor.org/stable/1774538.

Evenstar, L.A., Hartley, A.J., Stuart, F.M., Mather, A.E., Rice, C.M., Chong, G., 2009. Multiphase development of the Atacama Planation Surface recorded by cosmogenic He-3 exposure ages: Implications for uplift and Cenozoic climate change in western South America. Geology, 37(7), 658-658. https://doi.org/10.1130/G25437A.1.

Freitas, M.M.d., Paixão, R.W., Salgado, A.A.R., Eirado Silva, L.G., Cunha, P.P., Gomes, A.A.T., Martins, A.A., Almeida, J.C.H., Tupinambá, M.A., Dantas, M., 2022. The endorheic – Exorheic transition and later stage of fluvial incision in a wet tropical margin setting: The Atlantic draining Paraíba do Sul River basin (Brazil). Journal of South American Earth Sciences, 115, 103742. https://doi.org/10.1016/j.jsames.2022.103742.

Gouveia, M.P., Cunha, P.P., Falguères, C., Voinchet, P., Martins, A.A., Bahain, J.-J., Pereira, A., 2020. Electron spin resonance dating of the culminant allostratigraphic unit of the Mondego and Lower Tejo Cenozoic basins (W Iberia), which predates fluvial incision into the basin-fill sediments. Global Planet Change, 184, 103081. https://doi.org/10.1016/j.gloplacha.2019.103081

Guillocheau, F., Simon, B., Baby, G., Bessin, P., Robin, C., Dauteuil, O., 2018. Planation surfaces as a record of mantle dynamics: The case example of Africa. Gondwana Res., 53, 82-98. https://doi.org/10.1016/j.gr.2017.05.015.

Hu, Z.B., Li, M.H., Dong, Z.J., Guo, L.Y., Bridgland, D., Pan, B.T., Li, X.H., Liu, X.F., 2019. Fluvial entrenchment and integration of the Sanmen Gorge, the Lower Yellow River. Global Planet Change, 178, 129-138. https://doi.org/10.1016/j.gloplacha.2019.04.010.

Hu, Z.B., Pan, B.T., Bridgland, D., Vandenberghe, J., Guo, L.Y., Fan, Y.L., Westaway, R., 2017. The linking of the upper-middle and lower reaches of the Yellow River as a result of fluvial entrenchment. Quaternary Sci. Rev., 166, 324-338.

https://doi.org/10.1016/j.quascirev.2017.02.026.

Hu, Z.B., Pan, B.T., Guo, L.Y., Vandenberghe, J., Liu, X.P., Wang, J.P., Fan, Y.L., Mao, J.W., Gao, H.S., Hu, X.F., 2016. Rapid fluvial incision and headward erosion by the Yellow River along the Jinshaan gorge during the past 1.2 Ma as a result of tectonic extension. Quaternary Sci. Rev., 133, 1-14. https://doi.org/10.1016/j.quascirev.2015.12.003.

Huang, X., Wang, Y.N., Zhang, J., Wu, F.Z., Yang, Y.L., 2022. Low-temperature thermochronological insights into the Mesozoic-Cenozoic exhumation history of the Taihang-Lvliangshan region: A review. Geological Journal, 57(4), 1511-1529. https://doi.org/10.1002/gj.4352.

Jackson, S.E., Pearson, N.J., Griffin, W.L., Belousova, E.A., 2004. The application of laser ablation-inductively coupled plasma-mass spectrometry to in situ U-Pb zircon geochronology. Chem. Geol., 211(1-2), 47-69. https://doi.org/10.1016/j.chemgeo.2004.06.017.

King, L.C., 1953. Canons of landscape evolution. Geol. Soc. Am. Bull., 64, 721-752. https://doi.org/10.1130/0016-7606(1953)64[721:COLE]2.0.CO;2.

Kong, P., Jia, J., Zheng, Y., 2014. Time constraints for the Yellow River traversing the Sanmen Gorge. Geochem. Geophys. Geosyst., 15(2), 395-407. https://doi.org/10.1002/2013GC004912.

Li, J.J., 1991. The Environmental-Effects of the Uplift of the Qinghai-Xizang Plateau. Quaternary Sci. Rev., 10(6), 479-483. https://doi.org/10.1016/0277-3791(91)90041-R.

Li, J.J., 1999. In memory of Davisian Theory of erosion cycle and peneplain：a centurial study in China. Journal of Lanzhou University (Natural Sciences), 35(3), 157-163. https://doi.org/10.13885/j.issn.0455-2059.1999.03.018. (in Chinese, with English abstract)

Li, J.X., 2009. Discovery and geological significance of red clay in the Liulin section in the west part of Lvliang Mountains. ACTA Sedimentologica Sinica, 27(6), 1184-1190. https://doi.org/10.14027/j.cnki.cjxb.2009.06.017. (in Chinese, with English abstract)

Li, X.H., Liu, Y., Li, Q.L., Guo, C.H., Chamberlain, K.R., 2009. Precise determination of Phanerozoic zircon Pb/Pb age by multicollector SIMS without external standardization. Geochem. Geophys. Geosyst., 10. https://doi.org/10.1029/2009GC002400.

Li, Z.Y., Zhang, K., Liang, H., Chen, Z., Ma, Z.W., Xiong, J.G., Huang, P., 2022. Large river chronology along the Jinshaan Gorge on the Yellow River and its implications for initialization. Geomorphology, 400. https://doi.org/10.1016/j.geomorph.2021.108092.

Liang, H., Zhang, K., Li, Z., Fu, J., Yu, Z., Xiong, J., Li, X., Ma, Z., Huang, P., Li, Z., Zhang, Y., Hui, G., Tian, Q., Wang, W., Zheng, W., Zhang, P., 2022. How headward erosion breaches upstream paleolakes: Insights from dated longitudinal fluvial terrace correlations within the Sanmen Gorge, Yellow River. GSA Bulletin, 135(5-6), 1602-1617. https://doi.org/10.1130/B36537.1.

Licht, A., Dupont-Nivet, G., Pullen, A., Kapp, P., Abels, H.A., Lai, Z., Guo, Z., Abell, J., Giesler, D., 2016. Resilience of the Asian atmospheric circulation shown by Paleogene dust provenance. Nat. Commun., 7. https://doi.org/10.1038/ncomms12390.

Liu, C.H., Zhao, G.C., Sun, M., Zhang, J., He, Y.H., Yin, C.Q., Wu, F.Y., Yang, J.H., 2011. U-Pb and Hf isotopic study of detrital zircons from the Hutuo group in the Trans-North China Orogen and tectonic implications. Gondwana Res., 20(1), 106-121. https://doi.org/10.1016/j.gr.2010.11.016.

Liu, Q.S., Jin, C.S., Hu, P.X., Jiang, Z.X., Ge, K.P., Roberts, A.P., 2015. Magnetostratigraphy of Chinese loess-paleosol sequences. Earth-Sci. Rev., 150, 139-167. https://doi.org/10.1016/j.earscirev.2015.07.009.

Liu, S.W., Zhang, J., Li, Q.G., Zhang, L.F., Wang, W., Yang, P.T., 2012. Geochemistry and U-Pb zircon ages of metamorphic volcanic rocks of the Paleoproterozoic Luliang Complex and constraints on the evolution of the Trans-North China Orogen, North China Craton. Precambrian Res., 222, 173-190. https://doi.org/10.1016/j.precamres.2011.07.006.

Liu, Y.M., 2020. Neogene fluvial sediments in the northern Jinshaan Gorge, China: Implications for early development of the Yellow River since 8 Ma and its response to rapid subsidence of the Weihe-Shanxi Graben. Palaeogeogr. Palaeoclimatol. Palaeoecol., 546. https://doi.org/10.1016/j.palaeo.2020.109675.

Lu, H.Y., Zhang, H.Z., Feng, H., Wang, Y.C., Cai, D.X., Li, G.W., Lyu, H., Lei, F., Wang, K.X., Wang, S.M., Lai, W., Wang, X.Y., 2023. Landform evolution in Asia during the Cenozoic revealed by formation of drainages of Wei River and Indus River. Palaeogeogr. Palaeoclimatol. Palaeoecol., 619. https://doi.org/10.1016/j.palaeo.2023.111516.

Miao, X.D., Lu, H.Y., Li, Z., Cao, G.C., 2008. Paleocurrent and fabric analyses of the imbricated fluvial gravel deposits in Huangshui Valley, the northeastern Tibetan Plateau, China. Geomorphology, 99(1-4), 433-442. https://doi.org/10.1016/j.geomorph.2007.12.005.

Nie, J.S., Stevens, T., Rittner, M., Stockli, D., Garzanti, E., Limonta, M., Bird, A., Ando, S., Vermeesch, P., Saylor, J., Lu, H.Y., Breecker, D., Hu, X.F., Liu, S.P., Resentini, A., Vezzoli, G., Peng, W.B., Carter, A., Ji, S.C., Pan, B.T., 2015. Loess Plateau storage of Northeastern Tibetan Plateau-derived Yellow River sediment. Nat. Commun., 6.

https://doi.org/10.1038/ncomms9511.

Nie, J.S., Zhang, R., Necula, C., Heslop, D., Liu, Q.S., Gong, L.S., Banerjee, S., 2014. Late Miocene- early Pleistocene paleoclimate history of the Chinese Loess Plateau revealed by remanence unmixing. Geophys Res Lett, 41(6), 2163-2168. https://doi.org/10.1002/2014GL059379.

Orme, A.R., 2013. 1.12 Denudation, planation, and cyclicity: myths, models, and reality. Treatise on Geomorphology, 1, 205-232. https://doi.org/10.1016/B978-0-12-374739-6.00012-9.

Pan, B.T., Hu, Z.B., Wang, J.P., Vandenberghe, J., Hu, X.F., 2011. A magnetostratigraphic record of landscape development in the eastern Ordos Plateau, China: Transition from Late Miocene and Early Pliocene stacked sedimentation to Late Pliocene and Quaternary uplift and incision by the Yellow River. Geomorphology, 125(1), 225-238. https://doi.org/10.1016/j.geomorph.2010.09.019.

Pan, B.T., Hu, Z.B., Wang, J.P., Vandenberghe, J., Hu, X.F., Wen, Y.H., Li, Q., Cao, B., 2012. The approximate age of the planation surface and the incision of the Yellow River. Palaeogeogr. Palaeoclimatol. Palaeoecol., 356, 54-61. https://doi.org/10.1016/j.palaeo.2010.04.011.

Peng, H., Wang, J.Q., Liu, C.Y., Zhao, H.G., Huang, L., Zhao, X.C., Zhang, S.H., Liang, C., Wang, Z., Jiao, X.Q., Zhang, L., Zhang, T.B., Zhang, D.D., Zattin, M., Catto, S., 2023. Long-term and multiple stage exhumation of the Ordos Basin, western North China Craton: Insights from seismic reflection, borehole and geochronological data. Earth-Sci. Rev., 238. https://doi.org/10.1016/j.earscirev.2023.104349.

Peng, W.B., Nie, J.S., Wang, Z., Qiang, X.K., Garzanti, E., Pfaff, K., Song, Y.G., Stevens, T., 2018. A major change in precipitation gradient on the Chinese Loess Plateau at the Pliocene-

Quaternary boundary. J. Asian Earth Sci., 155, 134-138. https://doi.org/10.1016/j.jseaes.2017.10.031.

Peng, W.B., Zhang, H.B., Pullen, A., Li, M.T., Pan, B.T., Xiao, W.J., Nie, J.S., 2023. Stepwise increased spatial provenance contrast on the Chinese Loess Plateau over late Miocene-Pleistocene. Commun. Earth Environ., 4(1). https://doi.org/10.1038/s43247-023-00721-9.

Shang, Y., Beets, C.J., Tang, H., Prins, M.A., Lahaye, Y., van Elsas, R., Sukselainen, L., Kaakinen, A., 2016. Variations in the provenance of the late Neogene Red Clay deposits in northern China. Earth Planet. Sci. Lett., 439, 88-100. https://doi.org/10.1016/j.epsl.2016.01.031.

Shi, W., Dong, S.W., Hu, J.M., 2020. Neotectonics around the Ordos Block, North China: A review and new insights. Earth-Sci. Rev., 200. https://doi.org/10.1016/j.earscirev.2019.102969.

Slama, J., Kosler, J., Condon, D.J., Crowley, J.L., Gerdes, A., Hanchar, J.M., Horstwood, M.S.A., Morris, G.A., Nasdala, L., Norberg, N., Schaltegger, U., Schoene, B., Tubrett, M.N., Whitehouse, M.J., 2008. Plesovice zircon - A new natural reference material for U-Pb and Hf isotopic microanalysis. Chem. Geol., 249(1-2), 1-35. https://doi.org/10.1016/j.chemgeo.2007.11.005.

Souza, D.H., Parra, M., del Rio, I., Sawakuchi, A.O., Pupim, F.N., Hernandez-Gonzalez, J.S., Gomez, S., 2022. Late Quaternary Drainage Rearrangement Prevents the Vegetation Development in the La Tatacoa Intermontane Basin of the Colombian Andes. Front Earth Sc-Switz, 10. https://doi.org/10.3389/feart.2022.808718.

Stevens, T., Carter, A., Watson, T.P., Vermeesch, P., Ando, S., Bird, A.F., Lu, H., Garzanti, E., Cottam, M.A., Sevastjanova, I., 2013. Genetic linkage between the Yellow River, the Mu Us desert and the Chinese Loess Plateau. Quaternary Sci. Rev., 78, 355-368.

https://doi.org/10.1016/j.quascirev.2012.11.032.

Stevens, T., Palk, C., Carter, A., Lu, H.Y., Clift, P.D., 2010. Assessing the provenance of loess and desert sediments in northern China using U-Pb dating and morphology of detrital zircons. Geol. Soc. Am. Bull., 122(7-8), 1331-1344. https://doi.org/10.1130/B30102.1.

Strahler, A.N., 1950. Davis' concepts of slope development viewed in the light of recent quantitative investigations. Annals of the Association of American Geographers, 40(3), 209–213. https://doi.org/10.1080/00045605009352069.

Sun, J.M., Ding, Z.L., Xiao, W.J., Windley, B.F., 2022. Coupling between uplift of the Central Asian Orogenic Belt-NE Tibetan Plateau and accumulation of aeolian Red Clay in the inner Asia began at-7 Ma. Earth-Sci. Rev., 226. https://doi.org/10.1016/j.earscirev.2022.103919.

Vermeesch, P., 2012. On the visualisation of detrital age distributions. Chem. Geol., 312, 190-194. https://doi.org/10.1016/j.chemgeo.2012.04.021.

Vermeesch, P., 2013. Multi-sample comparison of detrital age distributions. Chem. Geol., 341, 140-146. https://doi.org/10.1016/j.chemgeo.2013.01.010.

Wang, X., Zhu, W.B., Ge, R.F., Luo, M., Zhu, X.Q., Zhang, Q.L., Wang, L.S., Ren, X.M., 2014. Two episodes of Paleoproterozoic metamorphosed mafic dykes in the Lvliang Complex: Implications for the evolution of the Trans-North China Orogen. Precambrian Res., 243, 133-148. https://doi.org/10.1016/j.precamres.2013.12.014.

Wiedenbeck, M., Alle, P., Corfu, F., Griffin, W.L., Meier, M., Oberli, F., Vonquadt, A., Roddick, J.C., Speigel, W., 1995. 3 Natural Zircon Standards for U-Th-Pb, Lu-Hf, Trace-Element and Ree Analyses. Geostandard Newslett., 19(1), 1-23. https://doi.org/10.1111/j.1751-908X.1995.tb00147.x.

Woolfe, K.J., Stewart, L.K., Francis, J.E., Arnot, M.J., 2000. PC99: a new freeware for manipulating and graphically displaying palaeocurrent data. Sediment Geol., 133(1-2), 1-5. https://doi.org/10.1016/S0037-0738(00)00034-8.

Xiao, G.Q., Sun, Y.Q., Yang, J.L., Yin, Q.Z., Dupont-Nivet, G., Licht, A., Kehew, A.E., Hu, Y.Z., Geng, J.Z., Dai, G.W., Zhao, Q.Y., Wu, Z.P., 2020. Early Pleistocene integration of the Yellow River I: Detrital-zircon evidence from the North China Plain. Palaeogeogr. Palaeoclimatol. Palaeoecol., 546, 0031-0182. https://doi.org/10.1016/j.palaeo.2020.109691.

Xiong, J.G., Li, Y.L., Zheng, W.J., Zhang, P.Z., Lei, J.H., Zhong, Y.Z., Hu, X., Li, Z.G., Gong, Z., Li, T., Zhang, Y.P., Xu, B.B., Tian, Q.Y., Xin, W.L., Ren, X.L., Yao, Y.F., 2018. Climatically driven formation of the Tangxian planation surface in North China: An example from northwestern Zhongtiao Shan of the Shanxi Graben System. Lithosphere, 10(4), 530-544. https://doi.org/10.1130/L720.1.

Xiong, J.G., Liu, Y.M., Zhang, P.Z., Deng, C.L., Picotti, V., Wang, W.T., Zhang, K., Liang, H., Zhao, X.D., Zhong, Y.Z., Liu, Q.R., Lei, J.H., Kang, H., Ren, Z.K., Zhang, H.P., Li, Y.L., 2022. Entrenchment of the Yellow River since the late Miocene under changing tectonics and climate. Geomorphology, 416. https://doi.org/10.1016/j.geomorph.2022.108428.

Xu, Y., Yue, L.P., Li, J.X., Sun, L., Sun, B., Zhang, J.Y., Ma, J., Wang, J.Q., 2009. An 11-Ma-old red clay sequence on the Eastern Chinese Loess Plateau. Palaeogeogr. Palaeoclimatol. Palaeoecol., 284(3-4), 383-391. https://doi.org/10.1016/j.palaeo.2009.10.023.

Yang, J., Nie, J.S., Garzanti, E., Limonta, M., Andò, S., Vermeesch, P., Zhang, H.B., Hu, X.F., Wang, Z., Zhao, B.J., Ncube, L., Stevens, T., Li, M.T., Li, H., Chen, T.A., Miao, Y.F., Pan, B.T.,

2021. Climatic Forcing of Plio- Pleistocene Formation of the Modern Limpopo River, South Africa. Geophys Res Lett, 48(14), e2021GL093887. https://doi.org/10.1029/2021GL093887.

Yue, L.P., Li, J.X., Zheng, G.Z., Li, Z.P., 2007. Evolution of the Ordos Plateau and environmental effects. Sci. China Ser. D., 50, 19-26. https://doi.org/10.1007/s11430-007-6013-2.

Zhang, H.Z., Lu, H.Y., Xu, X.S., Liu, X.M., Yang, T., Stevens, T., Bird, A., Xu, Z.W., Zhang, T., Lei, F., Feng, H., 2016. Quantitative estimation of the contribution of dust sources to Chinese loess using detrital zircon U-Pb age patterns. J. Geophys. Res. Earth Surf., 121(11), 2085-2099. https://doi.org/10.1002/2016JF003936.

Zhang, H.Z., Lu, H.Y., Zhou, Y.L., Cui, Y.Y., He, J., Lv, H.Z., Wang, K.X., Wang, X.Y., 2021. Heavy mineral assemblages and U-Pb detrital zircon geochronology of sediments from the Weihe and Sanmen Basins: New insights into the Pliocene-Pleistocene evolution of the Yellow River. Palaeogeogr. Palaeoclimatol. Palaeoecol., 562. https://doi.org/10.1016/j.palaeo.2020.110072.

Zhang, R., Nie, J.S., 2017. Goethite Concentration Variations in the Red Clay Sequence on the Chinese Loess Plateau. Geochem. Geophys. Geosyst., 18(11), 4179-4185. https://doi.org/10.1002/2017GC007148.

Zhao, G.C., Wilde, S.A., Sun, M., Li, S.Z., Li, X.P., Zhang, J., 2008. SHRIMP U-Pb zircon ages of granitoid rocks in the Luliang Complex: Implications for the accretion and evolution of the Trans-North China Orogen. Precambrian Res., 160(3-4), 213-226. https://doi.org/10.1016/j.precamres.2007.07.004.

Zhao, J.F., Liu, C.Y., Mountney, N., Lu, J.J., Cao, J.L., Yang, Y., Xue, R., 2016. Timing of uplift and evolution of the Luliang Mountains, North China Craton. Sci. China Earth Sci., 59(1), 58-69. https://doi.org/10.1007/s11430-015-5153-z.

Zhu, Y.M., Zhou, L.P., Mo, D.W., Kaakinen, A., Zhang, Z.Q., Fortelius, M., 2008. A new magnetostratigraphic framework for late Neogene Hipparion Red Clay in the eastern Loess Plateau of China. Palaeogeogr. Palaeoclimatol. Palaeoecol., 268(1-2), 47-57. https://doi.org/10.1016/j.palaeo.2008.08.001.

Figure (Color)

Click here to access/download;Figure (Color);Fig 1.jpg

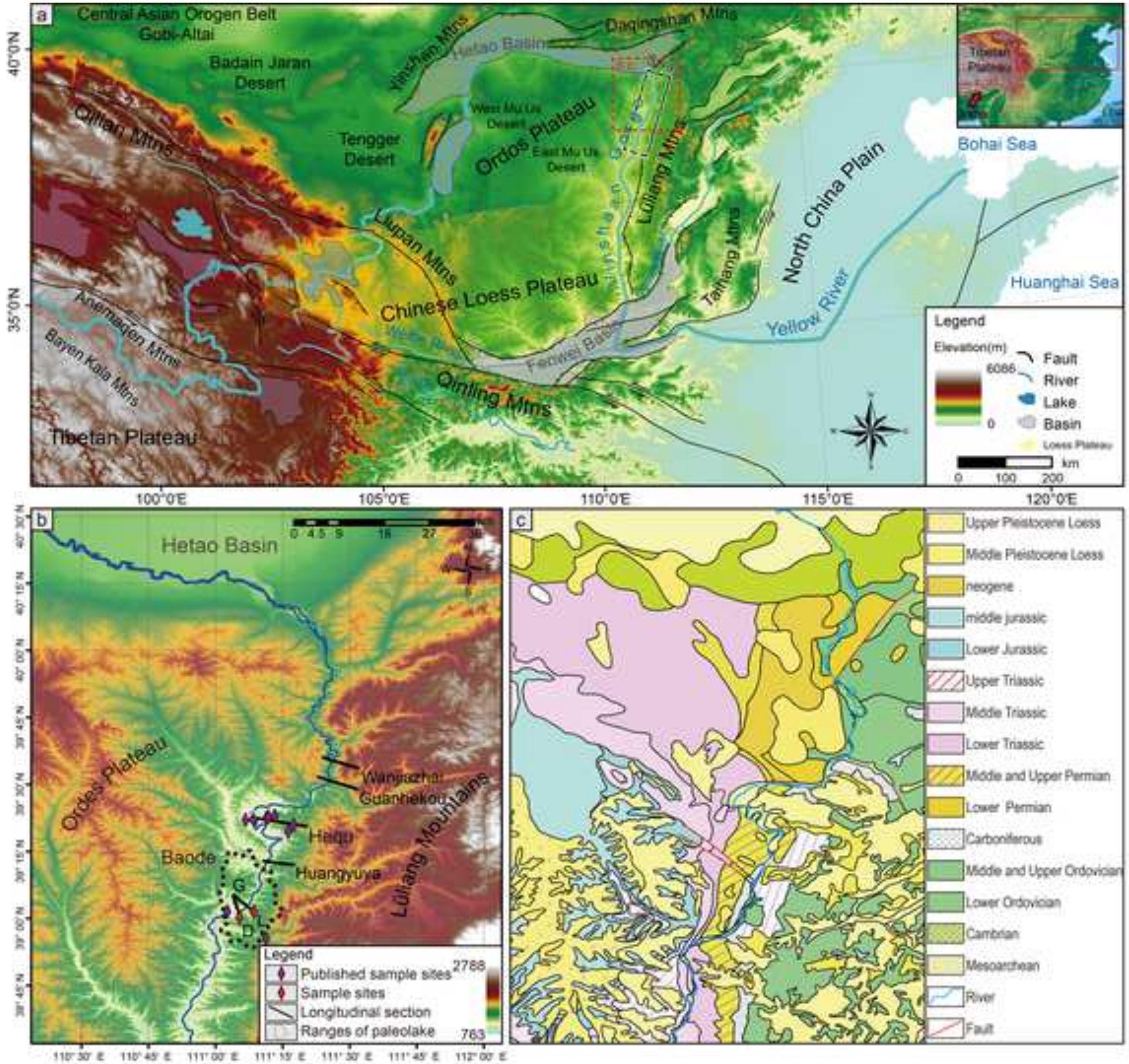

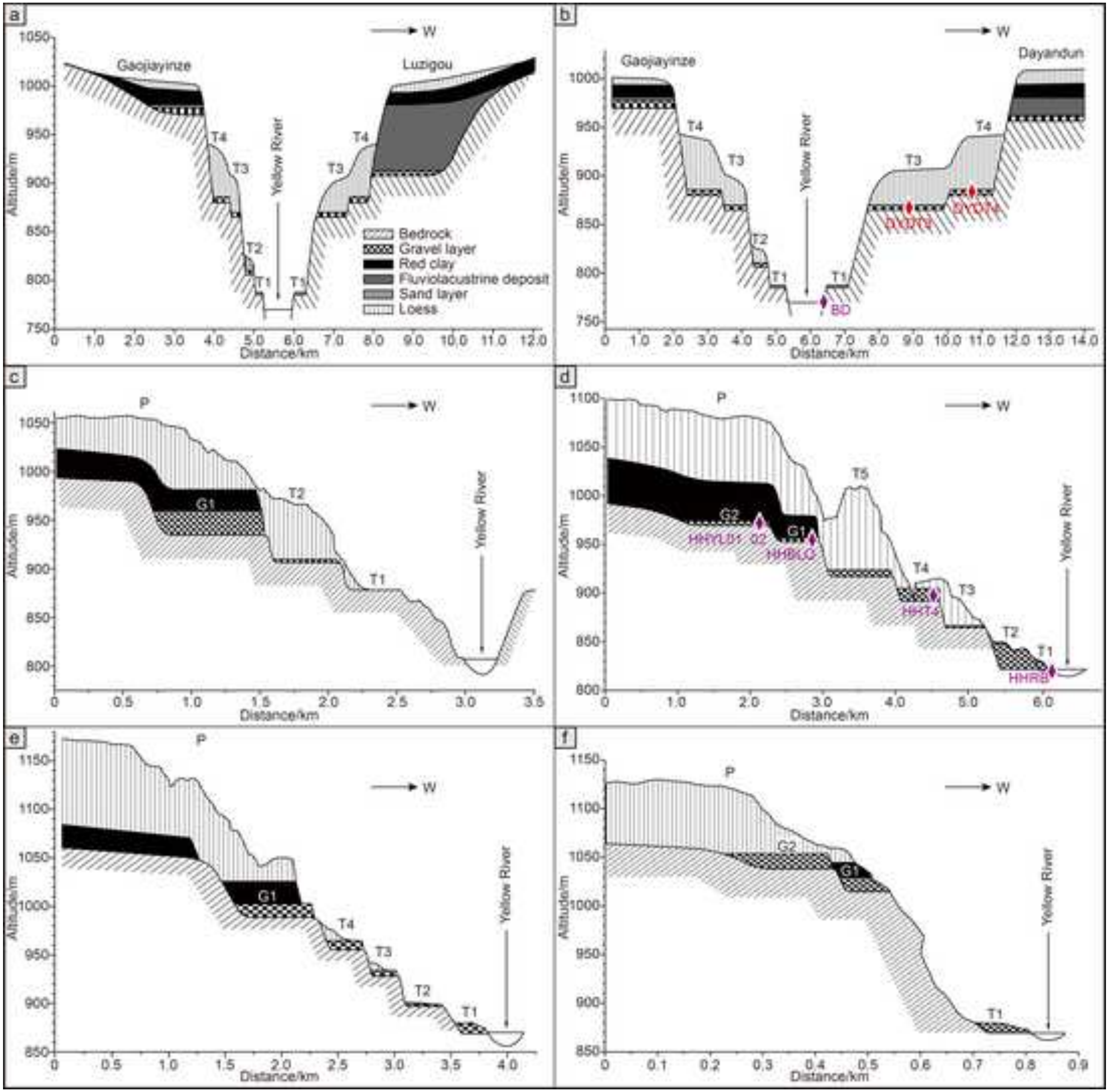
a
W
Gaojiayinze
Luzigou
T4
T3
T2
T1
Yellow River
Bedrock
Gravel layer
Red clay
Fluviolacustrine deposit
Sand layer
Loess
Altitude/m
Distance/km
b
Dayandun
BD
Yellow River
c
P
G1
d
T5
G2
HHYLD1
HHBLG
HHT4
HHRB
e
f

Figure (Color)	Click here to access/download;Figure (Color);Fig 3.jpg

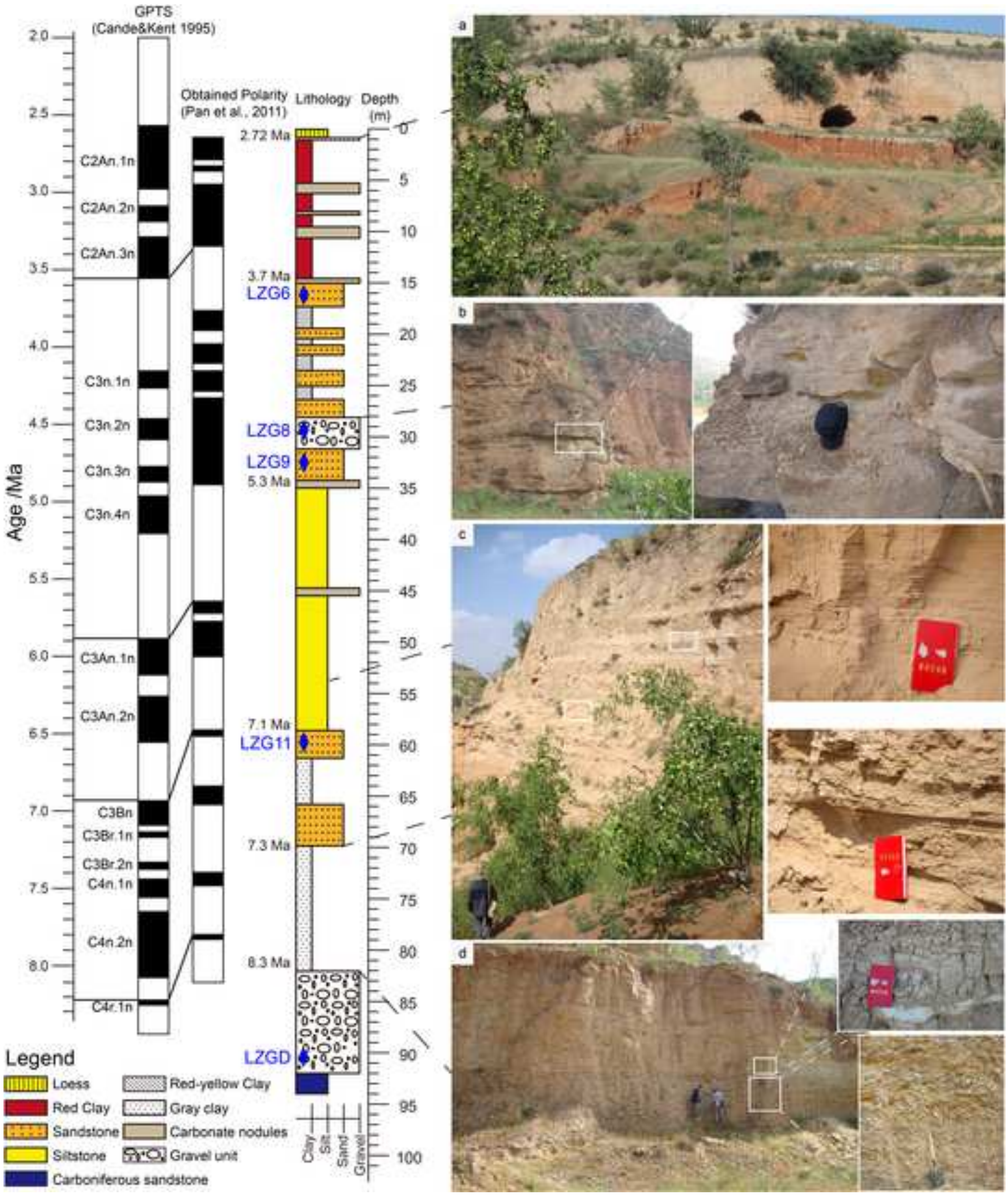

Figure (Color)   Click here to access/download;Figure (Color);Fig 4.jpg

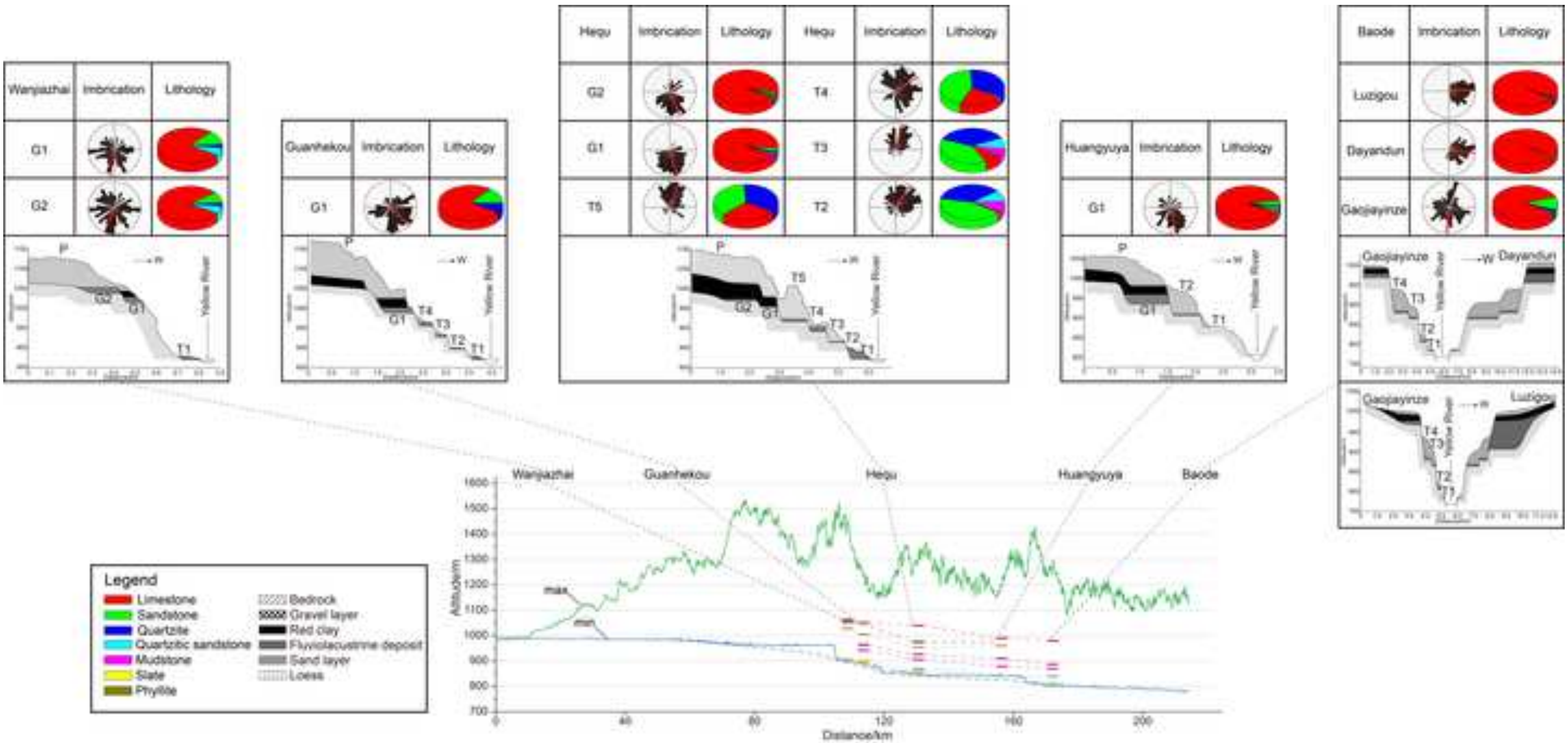

Figure (Color) Click here to access/download;Figure (Color);Fig 5.jpg

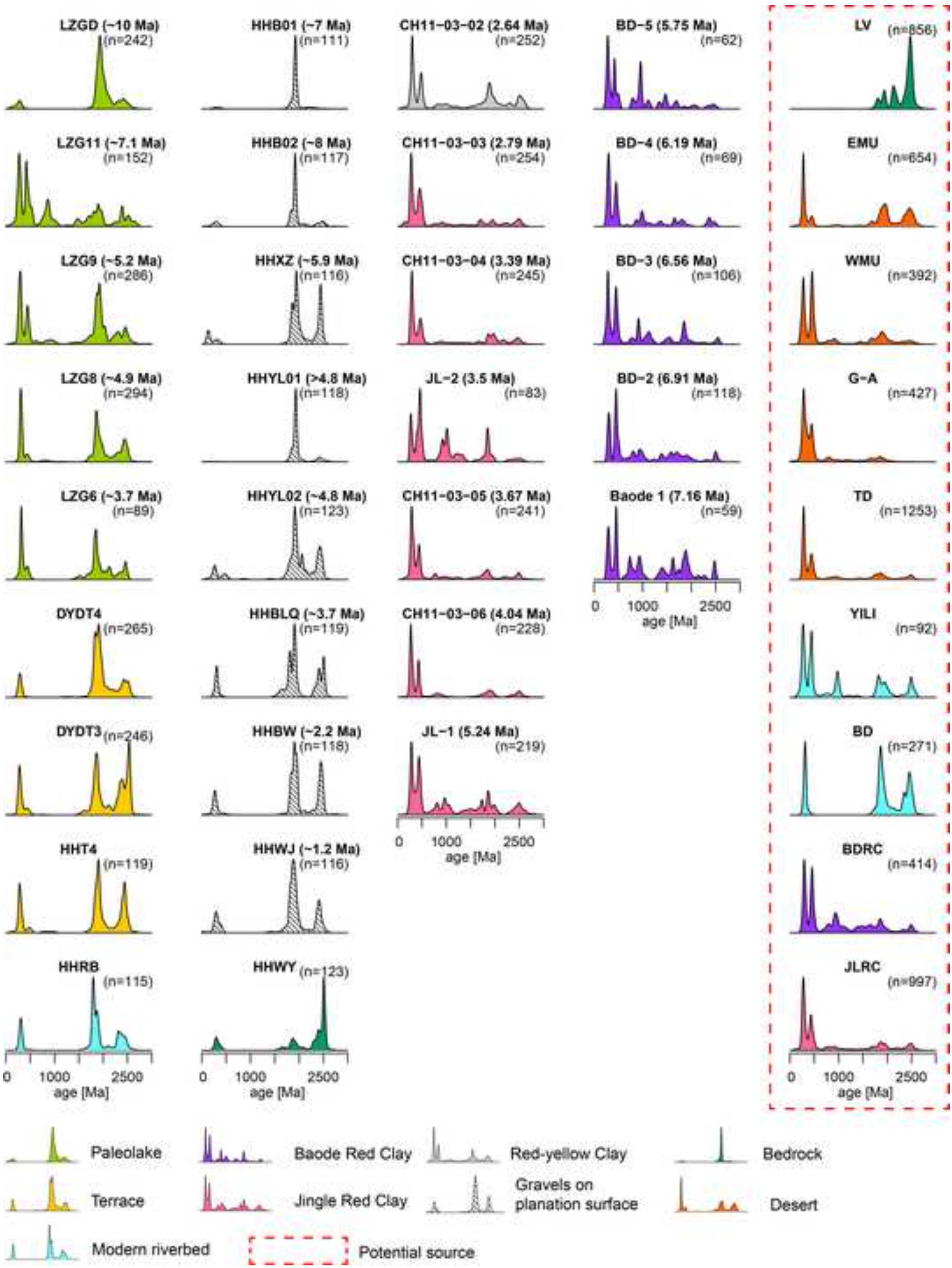

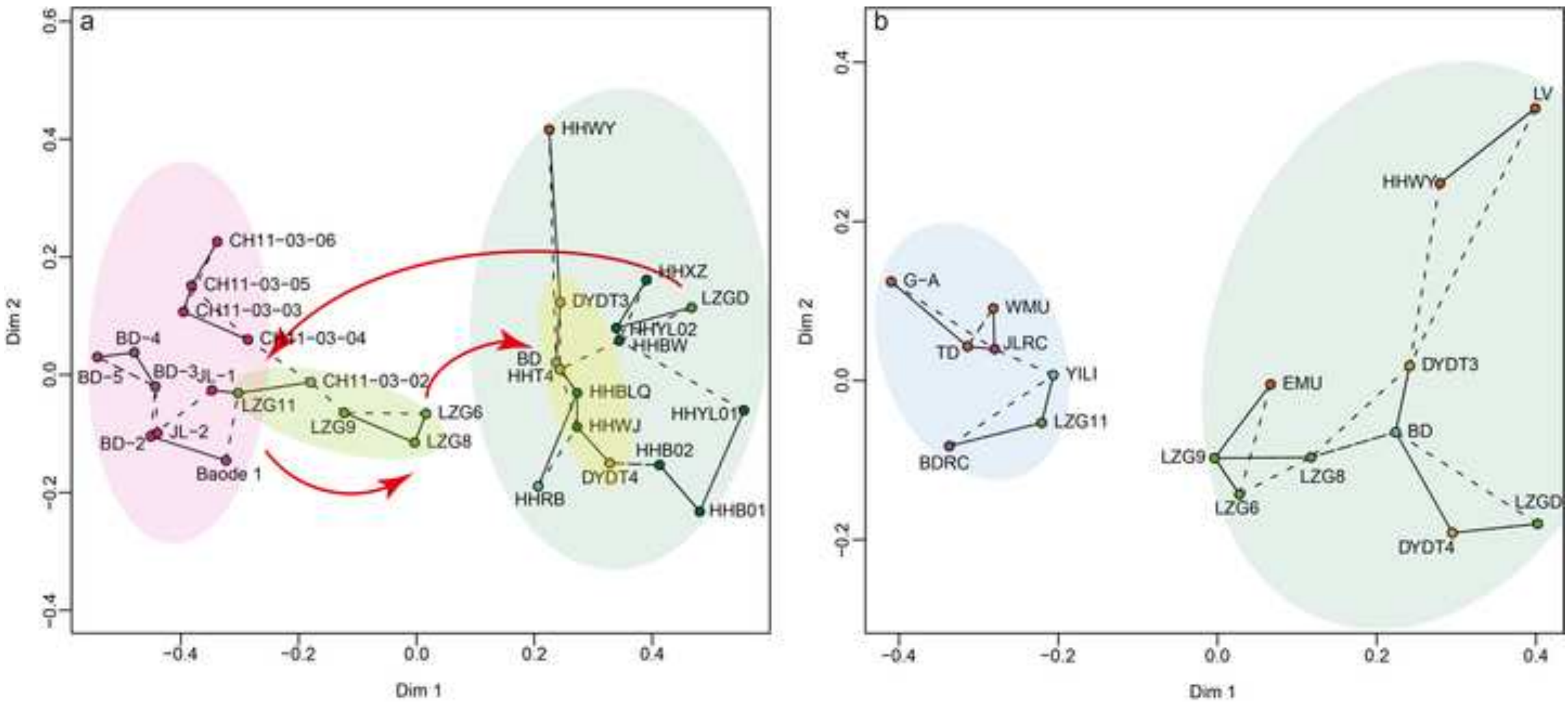
a
HHWY
CH11-03-06
CH11-03-05
CH11-03-03
CH11-03-04
HHXZ
DYDT3
LZGD
HHYL02
HHBW
BD-4
BD-5
BD-3
JL-1
CH11-03-02
BD
HHT4
HHBLQ
LZG11
LZG6
LZG9
LZG8
HHWJ
HHYL01
BD-2
JL-2
HHB02
Baode 1
DYDT4
HHRB
HHB01
Dim 1
Dim 2
b
LV
HHWY
G-A
WMU
TD
JLRC
YILI
DYDT3
EMU
LZG11
BD
BDRC
LZG9
LZG8
LZG6
LZGD
DYDT4

Figure (Color)

Click here to access/download;Figure (Color);Fig 7.jpg

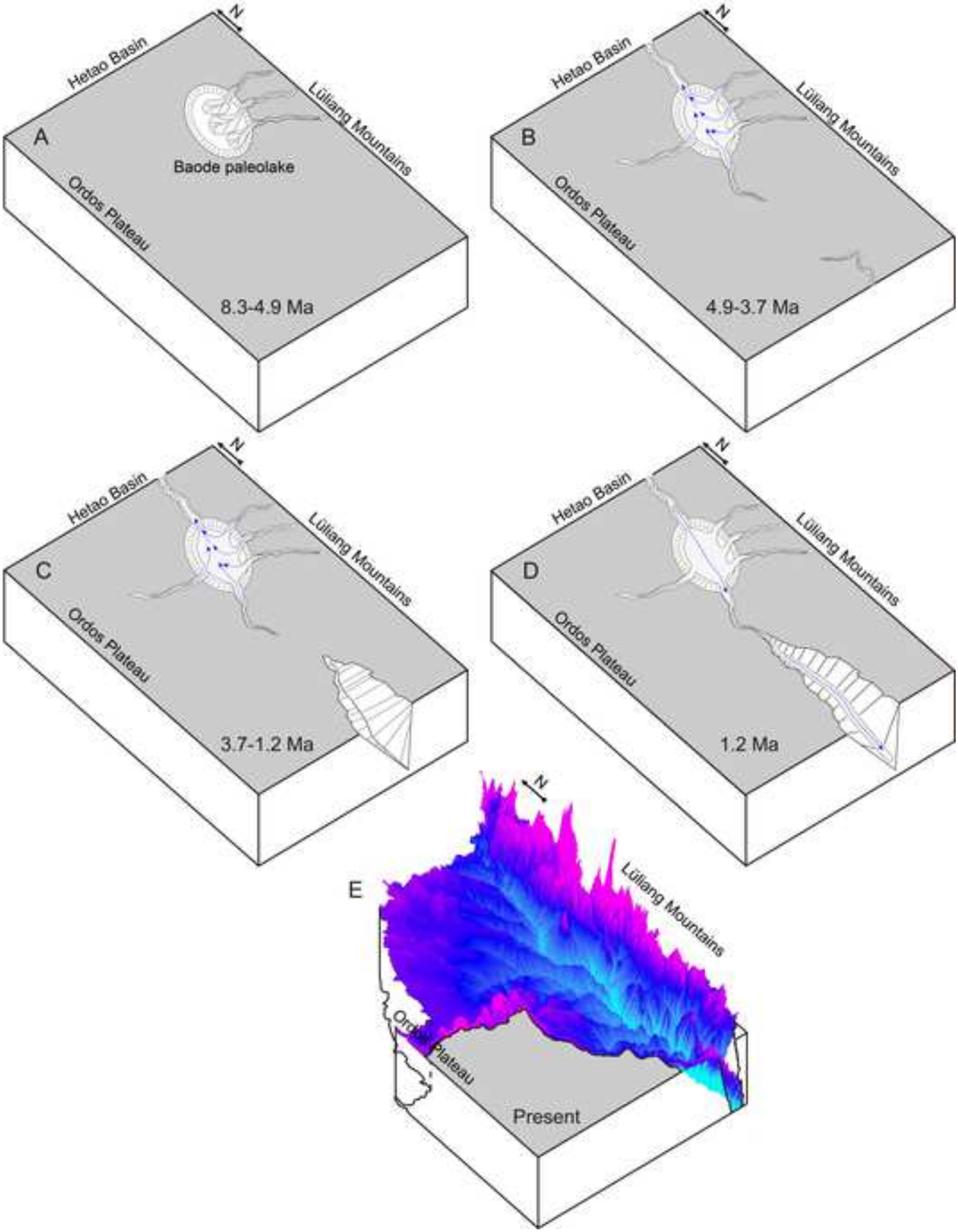

Click here to access/download
Supplementary material for online publication only
Sup 1.xlsx

Click here to access/download
Supplementary material for online publication only
renamed_122a1.xlsx

Declaration of interests

☐The authors declare that they have no known competing financial interests or personal relationships that could have appeared to influence the work reported in this paper.

☒The authors declare the following financial interests/personal relationships which may be considered as potential competing interests:

Zhenbo Hu reports financial support was provided by National Natural Science Foundation of China. Zhenbo Hu reports financial support was provided by Fundamental Research Funds for the Central Universities. Baotian Pan reports financial support was provided by State Administration of Foreign Experts Affairs.